Current Status and Future Trends of More Electric Cars' Power Systems

A. Emadi
Student Member, IEEE

A. V. Rajarathnam
Student Member, IEEE

M. Ehsani*
Fellow, IEEE

*corresponding author
Texas Applied Power Electronics Center
Department of Electrical Engineering
Texas A&M University
College Station, TX 77843-3128
Phone:(409)845-7582
Fax:(409)862-1976
E-mail:ehsani@ee.tamu.edu

Abstract- The More Electric Cars (MEC) concept is based on utilizing electric power to drive automobile subsystems which historically have been driven by a combination of mechanical, hydraulic, and electric power transfer systems. Increasing use of electric power (More Electric) is seen as the direction of technological opportunity for automotive power systems based on rapidly evolving technology advancements in power electronics, fault tolerant electrical power distribution systems, and electric-driven machines. This paper will address the fundamental problems faced in automotive power systems. Furthermore, a brief description of the conventional automotive power systems, their disadvantages, scope for improvement, future electric loads, advanced distribution system architectures, role of electronics and microprocessors, stability analysis, and current trends in automobile power system research will be given. Finally, this paper conclude with a brief outline of the advancement to be made in the future.

I. INTRODUCTION

The electrical systems in the early automobiles were introduced mainly for lighting, cranking, and battery charging purposes. But, in the recent years, electrical and electronic system components, circuits and accessories in an automobile have steadily increased, both in complexity and quantity. In addition, the electrical systems in a modern automobile perform more duties as some of the conventional mechanical loads are being replaced by electric loads [1]-[3].

The need for improvement in comfort, convenience, entertainment, safety, security, communications, and environmental concerns necessitates the need for improved electrical systems. This has motivated the research in restructuring the entire power system architecture in the automobiles [4]-[8].

At present most automobiles use a 12V DC electrical system with point-to-point wiring. Since the capability of this architecture in meeting the needs of future electrical loads is questionable, alternative architectures must be considered [4]-[6]. One way to simplify the architecture is by changing the control strategy [4]. Also, there is a need for advanced automotive power systems which includes multi-voltage level system, separate

power and signal buses, replacement of mechanical loads with electrical loads [5]-[7]. In [9] insertion of a DC/DC converter between the automobile battery and electrical loads is proposed. This would allow gradual conversion to higher battery voltage, regulation of DC distribution voltage, and multiple distribution voltage levels. However, a higher voltage system that is compatible with the current 12V DC architecture will be preferred during the transition to new system design [8]-[11].

There are opportunities in the following areas of the automotive power system - improved starting, integrated management of power generation and demand, higher system integrity, higher efficiency, and improvement of the vehicle electrical environment, giving benefit in component cost. These can be achieved by multi-voltage level system, a distribution architecture with a separate communication bus and replacement of some conventional, engine driven, mechanical loads with electric loads to provide an improved efficiency and packing flexibility among several advantages. There will be considerable increase in power requirements due to introduction of new functions like active suspension and catalyst preheater, and the electrification of the present functions like power steering and engine valves.

The role of power electronics in the automobiles will make significant impact in the future automobiles [3]. Further, the future for automotive electronics is bright. Electronic solutions have proven to be reliable over time and have enabled carmakers to solve problems otherwise unsolvable [12]-[15]. Now, it is obvious that electronics could provide the capability to solve automotive problems that defined conventional mechanical or electromechanical approaches [13]-[15]. On the other hand, microprocessor technology has become an essential technology for future automotive electronics. As advances in semiconductor technology allow more functions on a single chip, issues of reduced design cycle times have become a serious challenge [16].

This paper briefly discusses about the conventional automotive power systems, their disadvantages, scope for improvement, future electric loads, advanced distribution system architectures, role of electronics and microprocessors, stability analysis, current trends in automobile power system research and concludes with a brief outline of the advancement to be made in the future.

II. HISTORY OF AUTOMOTIVE POWER SYSTEMS

Electrical systems for vehicle lighting appeared about 80 years ago, using first 4V and then 8V batteries, which were charged from an external supply such as low tension radio batteries. When dynamos began to be fitted, at the beginning of the first world war, there were 6, 8 and 12V systems. Electric starting came into general use between the wars, and the car electrical system standardized on 12V-except for the Ford, which followed American practice and continued to use 6V into the 1950s. Cars with 6V systems had the starting problems: connectors that went open circuit, trafficators that had to be thumped on the door pillar to make them work and wiring that overheated.

In the 1960s, alternators were gradually introduced in place of dynamos, so that by 1975 they were a standard fitment. This allowed the use of a wide range of electrical accessories, ranging from heated rear windows to electrically driven radiator cooling fans. More recently, electronic fuel injection has added to the electrical load by requiring an

electrically driven fuel pump. Air conditioning adds to the electrical loads and is now being fitted to top models.

Diodes were the first solid state electronic device to be used in the automobiles. They accompanied the introduction of the alternator in the early 60's, and the application of transistors was extended to the regulator. It was not until the late 70's that the microprocessor was introduced, allowing the extensive use of sensors and controls to accommodate increasingly sever emissions and fuel economy regulations [1].

III. CONVENTIONAL AUTOMOTIVE ELECTRICAL SYSTEMS

Fig. 1 shows the conventional electrical distribution system for automobiles [2]. This has a single voltage level i.e., 12V DC, with the loads being controlled by manual switches and relays. This distribution network is a point-to-point topology in which all the electrical wiring aggregates at one or two fuse boxes from which it is distributed to different loads through relays and switches of the dashboard control. This kind of distribution network leads to expensive, complicated and heavy wiring circuits.

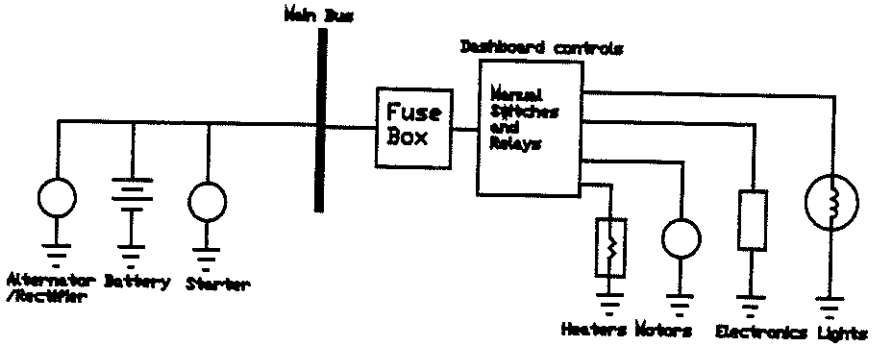

Fig. 1. Conventional 12V DC distribution system architecture

The present average power demand in an automobile is around 800W. The voltage in a 12V system actually varies between 9V and 16V, depending on the alternator output current, battery age and state of charge and other factors. The conventional electrical system in an automobile can be divided into the following subsystems.

A. Energy Storage System

Batteries are used in the automobiles for energy storage purposes. They are needed because the automobile requires a high quality power source for the vehicle to be independent and self starting. Their primary functions are to provide large current to crank the engine, supply electrical power for accessories for a reasonable period of time when the engine is not running or when the system demand exceeds that of generator/alternator output, and act as stabilizer, maintaining voltage levels for electrical distribution circuits.

Batteries commonly used in automobiles are the electro-chemical secondary cells in which the chemical reactions are reversible. Lead-acid batteries are commonly used because of their relatively low cost, high voltage per cell and good power capability, acceptable constant voltage charging characteristics, less or no maintenance, and their capability of delivering high currents in a short period of time. However, they have some

disadvantages: relatively low energy storage per unit weight, not very robust, poor performance at low temperatures , and explosive nature.

Experiments using a 20 Amps supply demonstrate just how dependent the battery is on the actual charging voltage. Typically, a car may require to be driven for either 500 or 100 miles to recharge its battery from 50% to 90% if the alternator output is held to either 13.2 or 14.0 volts. This effect shows how important it is for the charging circuit to be improved and any means of increasing the voltage at the battery considered.

Alternative batteries like Ni-Cd has better performance and life but are expensive. Also super capacitors are used in automotive applications. Their advantages include more rapid recharge and discharge capabilities, much larger life charge/discharge cycle life, and energy available directly measurable in terms of terminal voltage. However, they have certain limitations like high leakage current, failure modes and life expectancy yet to be determined, and cost unknown [10].

It seems there won't be any cost effectiveness for general energy storage other than the lead acid battery unless there is a drastic improvement in the development of new advanced battery technology.

In future cars equipped with electronic components we come into critical situations, when the battery state of charge is low and the voltage in the system breaks down during cold cranking. Beside of the possibility to protect every electronic part, like memories, by individual small batteries it seems to be more economic to think about a central small battery which is able to avoid a break-down of the voltage in the branches of the electrical network which contain sensitive parts [11]. This solution becomes even more advantageous when the amount of electronic equipment in standard cars is increasing. These batteries may be of nominal tensions below 12V, for example 8V, and contain only small capacities (Fig. 2).

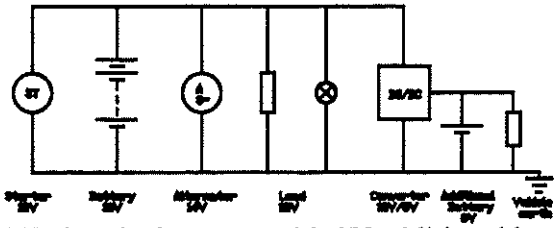

Fig. 2. 12V electrical system with 8V additional battery [11]

B. Charging System

Their primary task is to charge the battery while supplying electrical energy to operate other accessories. This is an integrated system of alternator, three-phase diode bridge rectifier and regulator. The voltage is regulated to a nominal of around 14.2V DC. The alternator used in automobiles has a poor characteristics with efficiency of around 50% and a high armature reactance. This means a poor fuel economy and the machine has to withstand a thermal stress of around 1.5kW. The high armature reactance implies that the stator core must be designed for unnecessary high flux for the terminal voltage, adding to cost and weight. Also, since the voltage has to be regulated at 14.2V DC independent of the speed, the machine capability is being restricted to low voltage output even at high speeds because of the system architecture. The present alternator can supply

effectively only up to 120A. With the increase in electrical loads in the future, a better design of the alternator is necessary.

The field circuit is energized by the battery at lower alternator speeds. The field relay is essential in those applications to prevent the battery from being discharged when engine is not in operation. Regulator operating current drawn from the battery is too low to cause a battery rundown. The regulator provides limiting by turning off the field current when the system voltage reaches a predetermined value. Some regulators provide temperature compensation that reduces the system voltage at high temperatures to reduce battery overcharge current.

C. Cranking System

This consists of a cranking motor, battery, control switches and interconnecting wiring. A typical 12/24V charging and 24V cranking system used in trucks is shown in Fig. 3. Cranking motors are DC series motors supplied by the battery which rotates the engine crankshaft through a pinion and flywheel ring gear. Cranking currents can be as high as 1600A with a peak reaching around 2500A for a fraction of a second at starting. This current is transferred from the battery through cables, terminals, and connectors. Resistance of this path has to be restricted to prevent excessive voltage drop that may result in malfunction of the motor. Control circuits that energize the motor include solenoid, switches and relays.

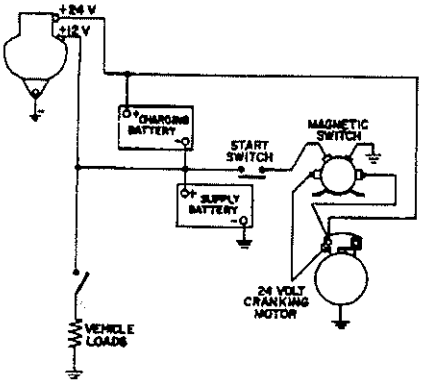

Fig. 3. Typical 12/24V charging and 24V cranking system for trucks [7]

D. Ignition System

The primary tasks of an ignition system are generating a voltage spike using the low battery voltage, delivering the voltage surge to each spark plug with correct timing to give maximum power, good fuel economy and low exhaust emissions, and establishing spark with enough intensity and for sufficient duration to ignite fuel/air mixture.

A typical 12V DC ignition system includes a battery charging system, a distributor with a shaft that runs at half the speed of the engine speed, a pulse transformer to transform the low system voltage to high voltage to establish an arc at the spark plugs, a secondary system with cables and insulation for high voltages. They must withstand deterioration due to high temperatures, moisture, oil, fuel, corona discharge etc., and spark plugs which place a gap in the combustion chamber between the center electrode and ground wires to ignite fuel mixture. The length and mass of the insulating material surrounding the

electrode which projects into the combustion chamber determines the spark plug heat range.

E. Lighting System

The majority of loads presently in a car are lamps. In terms of size, number of individual circuits and length of wire, the vehicle lighting system is by far the most extensive of all vehicle electrical sub-systems. These loads include head lamps, stop lamps, tail lamps, turn signal lamps, dashboard illumination, vehicle interior illumination, fog lamps, parking lamps, and warning lamps for emergency vehicles.

The trend is generally based on photometric regulation set by the government. Tungsten is the universal lamp filament material used for light source. It has high melting point and retains structural strength while incandescent lamps are nonlinear devices for which light output, life, color, and current depend on the voltage applied. They in life of the lamp with voltage is drastic. So it is important to maintain the voltage at the design value. The length of the filament depends on its diameter and voltage applied. Filament failure due to mechanical shock or vibration represents a large portion field problems today. Because short filaments are physically more rugged and optically easier to focus than long filaments, automotive applications favor low voltage tungsten lamps, and any future architecture will have to make 6V or 12V available for them. Headlamps, however, are seeing the introduction, on a limited basis, of High Intensity Discharge (HID) lamps [1]. These lamps require high striking voltages and electronic ballasting. Should their efficiency and optical advantages ever justify their high cost relative to tungsten lamps, they will represent a large market for power electronics.

F. Instrumentation System

Instrumentation in automobiles classified based on the functions include Fuel indicator, Temperature indicator, Speedometer, Pressure indicator, Ammeter and Voltmeter. According to their operating principles they can be classified as Mechanical or Magnetic.

Mechanical Instrumentation are mainly used for speed, temperature, and pressure measurement. Pressure and temperature gauges are usually based upon the bourdon tube or diaphragm as the basic operating principle. Speedometer uses the centrifugal force created to the rotating weights identical to a classical flyball governor provides action to move gearing and linkage. The electrical part this instrumentation is simply the illumination light required at the dashboard.

Magnetic Instrumentation include electro-magnetic devices which is based on the combined interaction of the current flow and magnetic fields. Since these type of gauges are connected to the sensor by means of wire, they provide flexibility in location and routing. Temperature sensors are thermistors which changes its resistance with temperature. Pressure sensors make use of mechanical diaphragm with a linkage that moves across a card containing coil of wires. Fuel gauges are similar with the float moving the linkage. Voltmeters and ammeters use the basic electro-magnetic principles for its operation. In the electro-magnetic gauges, temperature compensators are in-built through a resistive shunt that change with temperature.

G. Other Systems

The majority of loads presently in a car are motors and lamps. Motors present a somewhat different situation with lamps. At 12V, present motors loose 15% of their

energy in the brushes alone. In applications such as fans and blowers, where speed control and efficiency are important, but stall torque is not, brushless DC motors are an attractive alternative to brushed motors, especially at higher voltages. Where low speed, high torque is required, e.g., for window lifts and wipers, the ultrasonic motor with its low profile, pancake-like from-factor has recently been receiving attention [3]. Both the brushless and ultrasonic motors require power electronic drivers, and the cost and reliability of these drivers will influence considerably the large scale acceptance of the motors by the auto industry.

IV. FUTURE ELECTRICAL LOADS

In the future, throttle actuation, power steering, anti-lock braking, rear-wheel steering, and ride-height adjustment will all benefit from electrical power assistance, being compatible with electrical control systems, which are becoming essential to provide the ideal control function. For example, optimum fuel economy, performance and emissions cannot be achieved without interposing the fueling and ignition computer between the driver's foot and the throttle.

Many of the future electrical loads would replace existing engine power consumers, such as power-assisted steering and water and oil pumps, where the electrical drive can in fact require a lower engine power, being used only when needed. Some others are a response to government mandates, such as the electrically heated catalyst, and some are motivated by driver convenience, such as windshield.

However, there is a trend towards replacement of more engine driven mechanical loads with electrical loads due to regulatory measures, safety requirements, and driver's comfort. Some of the loads considered are air-conditioning system, active suspension system, electromechanical valve control, and electrically heated catalytic converter.

Also, DC motors with or without brushes will be used for applications like fans and pumps because of its efficiency at high voltage in addition to reduced cost, flexible control, high quality and reliability.

Most of future loads require power electronics controls. Indeed, power electronics will be used in future automobiles to perform two classes of functions. The first, which call a class I function, is the simple on/off control of loads now performed by mechanical switches and relays. This is a replacement function. The second, call a class II function, provides more sophisticated control of loads and requires a more complicated power electronic system, such as an inverter or DC/DC converter [2].

In aggregate these new loads represent an increase from the present average electric power requirement of more than 150%. Moreover, all of these loads would benefit from a voltage higher than 12V DC, and several, such as the electromechanical valves, active suspension and heated windshield, require substantially higher voltages.

V. POWERING UP A HIGHER SYSTEM VOLTAGE

As modern cars take in more and more electrical accessories, it may be time to consider increasing the base system voltage to cope with the greater loads. The optimum choice of voltage involves complex trade-off between cost, safety, economy, performance, and function. The most suitable voltage for one device will certainly not

suit all devices. A dual-voltage system is inevitable; in fact, three voltages may be necessary, as vehicles already have a separate 6V supply for instruments and electronic control units for engine management.

The most obvious choice for an increased voltage is that used on the larger commercial vehicles-24V. However, the rapid rise in electrical loads suggest that something higher than 24V could be needed in future.

Increased voltage benefits the starter commutator and brushgear, but, above about 50V, the increased number of armature conductors cancels this advantage and results in increased weight and cost. However, an increased system voltage, up to 50V, offers considerable reductions in the weight and cost. Switches and relays would carry lower currents so that voltage drops would cause less parasitic loss in the system. MOSFETs are now being used in solid state relays; although low cost devices are currently available only for 12 and 24V systems, demand for higher voltage devices is expected to make them available for 42V systems [8].

VI. ELECTRICAL DISTRIBUTION SYSTEM ARCHITECTURES

At present most Automobiles use a 12V electrical system with point-to-point wiring. The capability of this architecture in meeting the needs of future electrical loads is questionable. Furthermore, with the development of More Electric Vehicles (MEV) there is a greater need for better architectures.

A. Conventional Electrical Distribution System Architectures

Fig. 4 shows the conventional point-to-point automotive electrical distribution system [4]. Since the conventional architecture uses a 12V distribution and point-to-point wiring, the wiring harness is heavy and complex. The assembly process, therefore, becomes difficult and time consuming, leading to higher labor costs. Also retrofitting, fault tracing and repairing are more time consuming and expensive. The bulky harness also places constraints on the vehicle body design as the wires have to go through door hinges and other tight cavities. The large number of wires requires a proportionally large number of connectors; since the failure rate of connectors is high, system reliability is compromised. Fuses are needed to prevent fire in the wiring harness and must be placed in an easily accessible location. The conventional architecture has a central fuse box. Since this box contains all the fuse plugs, it is large and difficult to place. Furthermore, the fuse plugs are expensive. Another problem is that the system voltage varies over a wide range. As a result automotive loads have to be designed to function over a wide voltage range, making them heavy and expensive [4]. Also there is a problem of load-dump transient - a voltage spike caused due to sudden load loss on a fully loaded alternator. This requires overrated switches and loads for transients. Other disadvantages are: at 12V, motors losses about 15% of energy in the brushes alone and the 12V system cannot handle future electrical loads to be introduced in automobiles as it'll be expensive, heavy and inefficient.

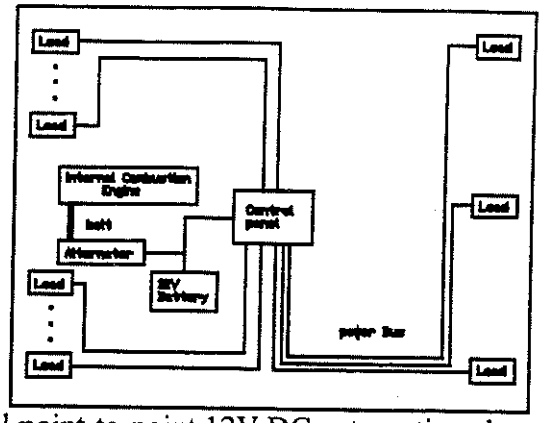

Fig. 4. The conventional point-to-point 12V DC automotive electrical distribution system

Changes in existing design may allow specialized designs to be used more effectively to improve overall cost reliability in an integrated system. On the other hand, there is a need for advanced automotive power systems which include multi-voltage level systems, separate power and signal buses, replacement of mechanical loads with electrical loads. These are motivated by the following factors:

- Continuing electrification of the automobile
- Currently 25% of a midsize car's fuel are used for electrical loads. If the some mechanical loads like air-conditioning and steering are electrified this percentage increases to about 50%. With these type of loads, power can be more effectively distributed and utilized at voltages much higher than 12V
- The automotive electricity is considerably expensive compared to the home electricity. Higher voltage levels improve electric efficiency by reducing ohmic losses and reducing copper requirement
- Improved electric efficiency reduces the automobile weight.
- Separate buses for signal and power
- Safety issues such as suspension, power steering, electric brakes, collision avoidance, back-up aide, and telematics
- Regulatory issues-higher fuel economy and lower emissions
- Interface between alternator and distribution system through power electronic circuits eliminates the need for overrated components
- The alternator can be allowed to generate unregulated voltage according to the varying engine speed, while the power conditioning circuit will provide a regulated, spike-free voltage
- Advance in the development of advanced power devices for cars capable of high-side switching, automatic shutdown on excessive temperature rise and integrated overcurrent protection
- Development power MOSFETs with low on-resistance
- Reduction in cost of power electronic component in the recent years

B. Advanced Electrical Distribution System Architectures

Since the conventional architecture does not adequately address the needs of a modern automobile, alternative architectures must be considered. One way to simplify the

architecture is by changing the control strategy [4]. In the conventional system each load is controlled by a dedicated wire. Alternatively a single wire multiplexed architecture can be used. In a multiplexed architecture the loads are controlled remotely by intelligent remote modules, as shown in Fig. 5. The control signal and power are sent through wires shared by many loads. Multiplexed topologies, therefore, reduce the number and length of wires in the harness. Furthermore, with communication between remote modules it will be practical to have a power management system, which can turn off unessential loads when there is not enough power. There are a number of multiplexed topologies, but the basic one are linear, star and ring.

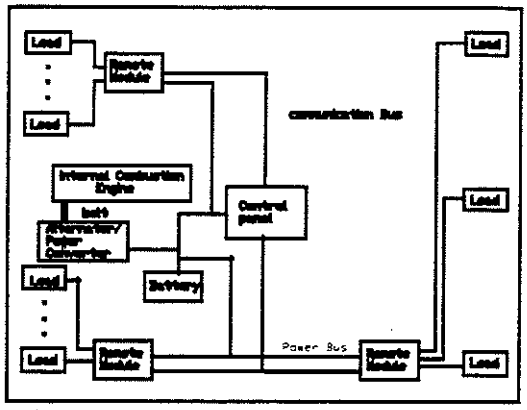

Fig. 5. Advanced automotive power system architectures of the future

A detailed diagram of a suggested advanced distribution system with high voltage level and medium frequency AC bus is shown in Fig. 6 [5]. Intelligent load control may avoid flat batteries by preventing lights left on, security system drains etc. This can be achieved by Power Management System (PMS). The primary functions of the PMS are battery management and charging strategy in a multiple battery system, load management, management of the alternator including the regulator, and provision and control of a high integrity supply system.

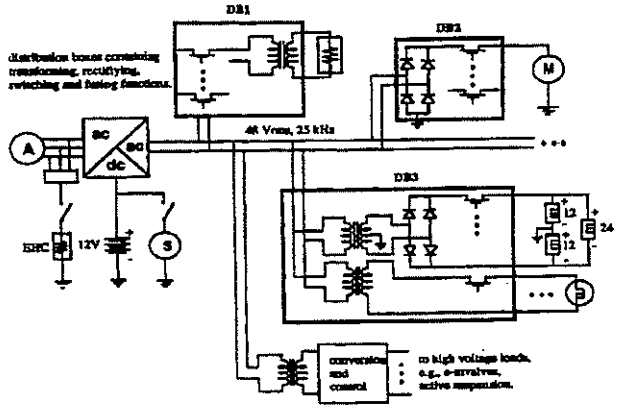

Fig. 6. High voltage, medium frequency AC distribution system

Distribution control networks simplifies vehicle physical design and assembly process and offer additional benefits from the amalgamation with intelligent power management control:

- They put all loads under intelligent control, therefore power management feature can be readily integrated into existing control with minimal cost
- Power management strategy can help optimize the size of the batteries and alternator
- Communications inherent with networked vehicle system can give improved performance with minimal increase in complexity and cost
- Vehicle economy can be improved using the knowledge of the battery state in a networked system

Further, the form in which power is distributed is important. A higher voltage will reduce the weight and volume of wiring harness. In addition, motor loads will be more efficient at higher voltages. A high voltage would also allow sheet-resistance based heated windshields, which require voltages greater than 60V, to be directly connected to the distribution bus. However, the advantage of a higher distribution voltage must be balanced against the cost of additional solution and shock protection, since voltage above 65V DC constitute a safety hazard [4]. Furthermore, lamps and electronics operate better at low voltage; hence in the case of a high voltage distribution bus it may be necessary to have a second low voltage bus. The main distribution can also be changed from DC to AC. The latter offers not only easy conversion to different voltage levels by the use of transformers, but also the ability to transfer power without contact. In this case, a DC power bus would also exist since a battery would be needed to start the engine and power essential loads when the engine is switched off.

In [9] insertion of a DC/DC converter between the automobile battery and electrical loads is proposed (Fig. 7). This would allow gradual conversion to higher battery voltage, regulation of DC distribution voltage, and multiple distribution voltage levels. Switching loss arising from parasitic inductance is a serious problem in this application. The nonlinear resonant switch can remove this source of loss, achieving zero current switching without sacrificing conduction loss or MOSFET switch utilization.

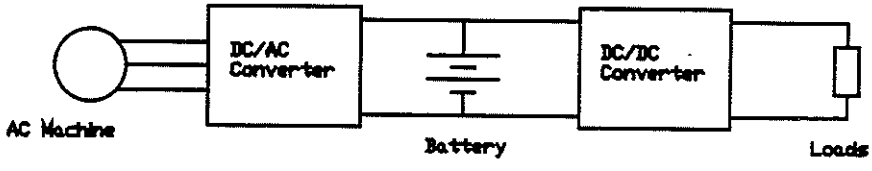

Fig. 7. New electrical system employing high-efficiency AC machine and isolated battery and load busses

The DC/DC load converter can provide the benefits of constant regulated voltage, higher automotive distribution voltage, and multiple load voltages. All of these benefits can considerably improve the automotive electrical system efficiency.

Also, it may be possible to improve the electrical system by replacing the components used in the conventional architecture. Permanent Magnet (PM) DC motors can be replaced by brushless DC, induction or variable reluctance motors. Similarly,

incandescent and halogen lamps can be replaced by more efficient and longer lasting High Intensity Discharge (HID) lamps [4]. Solid state relays can replace electromechanical relays, and fuse plugs can be replaced by fusing conductors or electronic fuses.

VII. THE ROLE OF ELECTRONICS AND MICROPROCESSORS IN ADVANCED AUTOMOTIVE ELECTRICAL SYSTEMS

In the early 1970s, other than radios and tape players, the only standard electronic components and systems on most automobiles were alternator diodes and voltage regulators. By the fall of 1974, there were twelve electronic system available, none of which were across the board standard production items. The twelve electronic systems were: alternator diodes, voltage regulators, electronic fuel injection, electronic controlled ignition, intermittent windshield wipers, cruise control, wheel lock control, traction control, headlamp control, climate control, digital clocks and air bag crash sensors [12].

The 1980s could be described as the decade of the emergence of automotive electronics. During this time the increase of electronic functions in passenger cars was quite dramatic. Among the first applications were the amplifier-type contact breaker ignition systems, then came breakerless units. Other systems include electronically controlled engine fueling, giving unprecedented performance or economy [13]. Electronic Anti-lock Braking Systems (ABS) are now becoming commonplace on highline cars, as are electronic instrumentation and driver information. Many more such functions are planned for future generations of cars, including electric actuation of brakes, steering and suspension.

Further vehicle functions can be implemented by the interaction of existing electronically controlled functions. One example of this type of interaction is in traction control where the ABS unit, on detecting wheel slip, can instruct the engine management unit to reduce engine torque until the car has recovered from the slip condition. Another example is the interaction between suspension, steering and braking controllers to maintain vehicle stability during braking and cornering. The interaction required can be achieved with dedicated links, but complexity and diagnosis advantages can be gained by the use of vehicle-wide local area networks, or data bus system [13].

Electronic engine management systems are becoming widely accepted, as is electronic ABS. Many more advanced systems are being planned. As roads become more heavily loaded, automotive electronic systems have their part to play in improving the safety and efficiency of road transport.

Reference [14] describes the electronically controllable system of valve actuation. It presents some performance predictions and results, and discusses some of the real life aspects of component performance requirements. The action of that system is referred to as Electronic Valve Timing (EVT). Valve motion has strong influence on the performance of diesel and spark ignition engines. The advantages of this relationship can be taken by designing valve motion to suit engines' application via EVT.

Current demands for shift comfort and driveability, and the need for interaction between the transmission and other vehicle electronic systems provide the impetus for introducing electronic control systems for transmission. The standard functions of such

systems have proven their worth and contributed towards satisfying these demands. For this reason, despite the additional cost involved, most automatic transmissions will be electronically controlled within next years. This is not only aimed at improving comfort and drivebility, but also at reduction fuel consumption, especially as automatic transmissions have always come off worse in tests than manual transmissions in this respect [15].

The future for automotive electronics is bright. Electronics solutions have proven to be reliable over time and enabled carmarkers to solve problems otherwise unsolvable. Some other predictions for the future are:

- Expansion of the airbag system to include side impact protection
- Magnetic transistors and diodes that can be directly integrated with signal conditioning circuits
- Electronic switched stop lamps involving a rate-of-closure detector system to determine if the vehicle's speed is safe for objects ahead of it. If the closure rate is unsafe, the stop lights could be activated to alert trailing drivers to a pending accident
- The integration of watchdog and fail-safe functions onto a microcontroller
- Microcontrollers that operate at frequencies of 24MHz or 32MHz to allow more code to be executed in the same amount of time
- A move from switching units to stepped operation actuators and the substitution of continuous for discrete time control
- Electroheological and magnetorheogical fluid actuators
- Micromechanical valves as actuators for converting low control power as in regulating the flow of fluids in hydraulic or pneumatic systems

After the introduction to automotive electronics in the 1970's, microprocessor-based automotive technology matured quickly in the 1980's. Now, it is clear that microprocessor technology has become an essential technology for future automotive electronics. It provides for automotive designers and engineers the opportunity to solve many problems and the unprecedented flexibility to innovate beyond mechanical limitations.

Newer architectures such as the Reduced Instruction Set Computer (RISC) and the Digital Signal Processor (DSP) promise higher levels of performance and, thereby, open the doors for new applications. DSP application to the exhaust will soon enable more efficient operation by cancellation of exhaust output pressure wave. In the future, microprocessor could alter engine mount characteristics in real time to reduce the coupling of engine vibration to the vehicle chassis. DSP technology already sophisticated dynamic suspension controls for high-performance cars and will soon be practical for most vehicles.

Microprocessor systems can accurately modify spark timing to optimize engine performance at all engine speeds. Also, they can eliminate the carburetor by direct control of fuel injection, the distributor contact points by use of a magnetic flux sensor, and the distributor itself by direct control of spark advance for each cylinder. A next logical step will eliminate the cam and all of its associated bearings, rods, and adjustments by

electronic control of valve openings and closings, producing an engine fully controlled by electronics.

Microprocessor technology makes it possible to explore engine technologies that were previously considered impractical for cars. Reasonable mechanical control systems could not produce adequate fuel economy or pollution reduction from two-cycle engines. Using leading edge microprocessor technology, an Australian company has produced a practical two-cycle engine that is suitable for a passenger car. This engine is much smaller than a traditional four-cycle engine of comparable horsepower [16].

In a few cars now, and in most future cars, microcontrollers will pass command signals over high speed serial data links using standardized communications protocols. Multiplexed wiring uses microprocessor technology to drastically reduce the amount of copper wiring, interconnection, and mechanical hardware in the car [16].

VIII. STABILITY ANALYSIS

There are many definitions of stability when considering linear, non-linear, discrete, and continuous systems. Linear system stability analysis is commonly performed using Routh-Hurwitz, root locus, Bode plot methods, and the Nyquist criterion. Another well known method of providing linear or non-linear system stability is the use of Lyapunov's second method [17]. Difficulty arises, however, in developing Lyapunov functions for many non-linear systems. Thus in determining the stability of a large system, more state-specific definitions are desirable. Stability considerations in non-linear systems require the consideration of initial conditions, external inputs, and their effects on non-linear components of the system. No known general analytical approach for the solution of non-linear systems is presently available.

The definition of stability in this paper considers the asymptotic stability as in the case of Lyapunov. However, we will not search for a suitable Lyapunov function, but instead consider the conditions of voltages and currents on the inputs and outputs of the subsystems. One form of instability is the divergence of one or more of these input or output voltages or currents (signals) from a desired value to some value which is outside the zone of tolerance, and the failure of the signal to return to within the zone of tolerance within a predefined period of time, i.e. unboundedness.

The common approach is to develop small signal linearized equivalent circuits and simulate the system to determine system stability. System stability is thus defined as the absence of instabilities on the main nodes. This linearized method governs small signal stability of the integrated system, but do not guarantee large signal stability for the entire system. For large signal stability, it is important to explicity include two other techniques in designing and building an automotive power system. Computer analysis and hardware testing form the other legs of a stability trial which should always be applied to the development of a complex system.

Large-signal stability refers to the ability of the system to move from one steady state operating point following a disturbance to another steady state operating point. Of prime concern is the way that the automotive power system will respond to dynamics caused by interconnecting between equipments and also to both a changing power demand and to various types of disturbance (loss of generation, short circuits, open circuits, etc).

However, for large-signal stability studies, time domain simulations using reliable large-signal models are inevitable. It depends on the actual control and protection circuit dynamics which may include, but is not limited to undervoltage lookout, overvoltage and overcurrent protections, cycle-by-cycle limiting, and nonlinearities due to magnetic saturation, leakage, semiconductor operation, temperature variations, aging, and castostrophic failures.

The stability of an automotive power system can be enhanced, and its dynamic response improved, by correct system design and operation. For example, the following features help to improve stability:

- the use of protection equipments that ensure the fastest possible fault clearing
- the use of a system configuration that is suitable for the particular operating conditions (e.g. avoiding long, heavily loaded links)
- ensuring an appropriate reserve in power capacity
- avoiding operating the system at low voltage
- avoiding weakening the network by the simultaneous outage of a large number of loads

In practice, financial considerations determine the extent to which any of these features can be implemented and there must always be a compromise between operating a system near to its stability limit and operating a system with an excessive reserve of generation and transmission. The risk of losing stability can be reduced by using additional elements inserted into the system to help smooth the system dynamic response.

IX. CONCLUSIONS

There is no doubt that the automobile power system architecture is heading for a drastic change which is imminent. Recent advances made in the area of power electronics, electric drives, electronic control, microprocessors, and microcontrollers are already providing the impetus to improve the automobile electrical and electronic systems. The extent of this change will certainly depend on the cost effective production of power electronics and other automotive electric components. The future automotive power systems will employ multi-voltage level systems, separate buses for power and communication, and an intelligent load management system. There is no question that power electronics will play an increasingly important role in automotive electrical systems. The extent of this role will be determined by how successful the power electronics industry is in producing apparatus at costs competitive with the alternatives. Electronic engine management systems will become widely accepted and automotive electronic systems, microprocessors and microcontrollers will have their considerable part to play in improving the efficiency and safety of automobiles.

REFERENCES

[1] J. G. Kassakian, H. Wolf, J. M. Miller, and C. J. Hurton, "The future of automotive electrical systems," *Proc. of IEEE Workshop on Power Electronics in Transportation*, Dearborn, Oct. 1996, pp. 3-12.

[2] J. G. Kassakian, "The future of power electronics in advanced automotive electrical systems," *Proc. of IEEE Power Electronics Specialist Conf.*, 1996, pp. 7-14.

[3] L. A. Khan, "Power electronics in automotive electrical systems." *Proc. of IEEE Workshop on Power Electronics in Transportation*, Dearborn, Oct. 1996, pp. 29-38.
[4] K. K. Afridi, R. D. Tabors, and J. G. Kassakian, "Alternative electrical distribution system architectures for automobiles," *Proc. of IEEE Workshop on Power Electronics in Transportation, Dearborn*, Oct. 1994, pp. 33-38.
[5] J. G. Kassakian, H. C. Wolf, J. M. Miller, and C. J. Hurton, "Automotive electrical systems-circa 2005," *IEEE Spectrum*, pp. 22-27, Aug. 1996.
[6] J. M. Miller, "Automotive power systems: present and future technologies," *Seminar at Texas A&M University*, Oct. 1997.
[7] E. Heller, "Truck electrical systems," *SAE 23rd L. Ray Buckendale Lectures*, 1997.
[8] J. G. W. West, "Powering up - a higher system voltage for cars," *IEE Review*, pp. 29-32, Jan. 1989.
[9] S. W. Anderson, R. W. Erickson, and R. A. Martin, " An improved automotive power distribution system using nonlinear resonant switch converters," *IEEE Trans. on Power Electronics*, vol. 6, no. 1, Jan. 1991, pp. 48-54.
[10] A. G. A. Guthrie, "The size of batteries to come," *IEE Colloquium on Vehicle Electrical Power Management and Smart Alternators*, 1988.
[11] R. Aumayer and G. L. Penna, "Batteries for new concepts of electrical systems in passenger cars," *IEE Colloquium on Vehicle Electrical Power Management and Smart Alternators*, 1988.
[12] R. Jurgen, *Automotive Electronics Handbook*, McGraw-Hill Inc., 1994.
[13] C. R. Boyce, "Automotive local area networks," *IEE Computing & Control Engineering Journal*, pp. 128-130, May 1990.
[14] M. E. Behr, "Potential for lost motion electronic valve timing," *Proc. of the International Congress on Transportation Electronics*, Oct. 1990, pp. 325-333.
[15] M. Schwab, "Electronically controlled transmission systems - current position and future developments," *Proc. of the International Congress on Transportation Electronics*, Oct. 1990, pp. 335-342.
[16] M. A. Goldman, S. E. Groves, and J. M. Sibigtroth, "The role of microprocessors in future automotive electronics," *Proc. of the International Congress on Transportation Electronics*, Oct. 1990, pp. 121-130.
[17] R. E. Kalman and J. E. Bertram, "Control system analysis and design via the second method of Lyapunov: I. continuous time systems," *American Society of Mechanical Engineering*, 1960.

Advantages of Switched Reluctance Motor Applications to EV and HEV: Design and Control Issues

K. M. Rahman, Student Member, IEEE
B. Fahimi, Student member, IEEE
G. Suresh, Student Member, IEEE
A. V. Rajarathnam, Student Member, IEEE
M. Ehsani, Fellow, IEEE

Texas A&M University
Department of Electrical Engineering
College Station, TX 77843-3128

Abstract- **Land vehicles need their drivetrain to operate entirely in constant power in order to meet their operational constraints, such as initial acceleration and gradability, with minimum power rating. The internal combustion engine (ICE) is inappropriate for producing this torque-speed profile. Therefore, multiple gear transmission is necessary with the ICE in a vehicle. Some electric machines, if designed and controlled appropriately, are capable of producing an extended constant power range.**

The purpose of this paper is to investigate the capabilities of switched reluctance motor (SRM) for EV and HEV applications. This investigation will be carried out in two steps. The first step involves the machine design and the finite element analysis to obtain the static characteristic of the motor. In the second step, the finite element field solutions are used in the development of a nonlinear model to investigate the dynamic performance of the designed motor. Several 8-6 and 6-4 SRM geometries will be investigated. Effects of different stator and rotor pole widths and pole heights on the steady state as well as on the dynamic performance of the motor will be studied. The air gap for each motor will be made as small as manufacturally possible. The performances to be compared for each design motor are, i) the range of the constant power operation, ii) drive efficiency in this extended constant power range, iii) the power factor in this operational range, and iv) the short time overload capability. The first performance index defines the rated power of the motor. Longer the constant power range lower is the power rating for the same vehicle performances. Hence, special emphasis will be given on this. In the high speed operation of the SRM, there will be considerable phase overlapping. Hence, thicker back iron than usual might be needed to prevent the back iron from saturating. However, since flux peaking of each phase occurs at different rotor positions, the phase overlapping might not necessitate special designing of the back iron. However, the possibility of back iron being saturated will not be neglected and will be investigated. The optimal control parameters of SRM, which maximize the constant power range with maximum torque per ampere, will be calculated. Performance comparison will be made for this optimal operation. Simulation results of the designed SRM will be presented for vehicle acceleration. To demonstrate SRM's capability in producing an extended constant power range, experimental results will be presented, however, for a reduced size motor available commercially.

I. INTRODUCTION

Switched reluctance motor (SRM) is gaining much interest as candidate for Electric Vehicle (EV) and Hybrid Electric Vehicle (HEV) electric propulsion for its simple and rugged construction, ability of extremely high speed operation, and hazard free operation. In view of these characteristics, one of the early SRMs was designed and built for electric vehicle application [1]. In designing this SRM, the major attention was given on the efficiency of the drive. Later, an optimized design method of SRM was reported in [2] for EV application. The design optimization was based on static analytical model of SRM, similar to the one developed by Corda and Stephenson [3]. Moreover, the efficiency optimization was carried out for the constant speed operation of the drive with non-optimal control. Like the previous design, the special emphasis was given in this design on the drive efficiency and additionally on the drive cost. Most recently, a 100 hp SRM was designed and built in [4] for electric vehicle application. No special control scheme, design method, or optimization technique were, however, presented.

While designing an SRM in all the previous methods, no attention was given to the vehicle dynamics. Vehicle dynamics dictate a special torque-speed profile for its propulsion system. Our recent study has shown that, a vehicle, in order to meet its operational constraints such as initial acceleration and gradability with minimum power, needs the powertrain to operate entirely in constant power [5]. The power rating of a motor that deviates from the constant power regime can be as much as two times that of a motor operating at constant power throughout its speed range in a vehicle. Operation entirely in constant power is not possible for any practical drive. An extended constant power range is, however, possible if the motor is appropriately designed and its control strategy is properly selected.

This paper will investigate the capabilities of SRM for vehicle traction. For this purpose, several SRMs will be designed and their optimal control parameters, which maximize the constant horse power range, will be calculated. A 2-D finite element analysis will be used to obtain the static characteristics of designed motors. The finite element field solutions will be then used in the development of a nonlinear model to investigate the steady state and the dynamic performance of the designed motors. The nonlinear model will also be used to search for the optimal control parameters (turn-on and turn-off angles) of each designed SRM which

extends the constant power range with maximum torque per ampere. Performance comparison will be made for this optimal operation. Several 8-6 and 6-4 SRM geometries will be investigated. Effects of different stator and rotor pole geometries on the steady state as well as on the dynamic performance of the motor will be studied. In the high speed operation of the SRM, there will be considerable phase overlapping. Hence, thicker back iron than normal might be needed to prevent it from saturating. However, since flux peaking of each phases occur at different rotor positions, the phase overlapping might not bring the back iron into saturation. However, the possibility of back iron being saturated will not be neglected and will be investigated. Besides the range of the constant power operation, the other performances which will be investigated for each designed motor are, i) the drive efficiency in this extended constant power range, ii) the power factor in this operational range, and iii) the short time overload capability. Simulation results of the designed SRMs in vehicle acceleration will be presented. To demonstrate that the SRM is capable of producing a long constant power range when controlled optimally, experimental results will also be presented, however, for a reduced size motor available commercially.

II. SRM STATIC CHARACTERISTICS

To investigate the dynamic and steady state performances of each SRM geometry considered in this paper, the static torque and flux linkage characteristics as functions of stator current and rotor position are required. The non-linearity of the SRM owing to its saturation region of operation, however, complicates the analysis. Several non-linear analytic models of SRM are presented in the literature to obtain the static data [3,6-8]. For accuracy we will, however, rely on the finite element analysis to obtain the static data. Finite element analysis will be performed on several 6-4 and 8-6 SRM geometries with varying stator and rotor pole widths and heights. Later, the static torque and flux linkage data obtained from the finite element analysis will be used in the dynamic model to determine the drive performance with optimal control parameters.

III. NON-LINEAR SRM MODEL

A block diagram of the non-linear SRM model is shown in Fig. 1. The static flux linkage and torque data as functions of the stator current and rotor position, obtained from the finite element analysis for each SRM geometry, are used in the dynamic model in order to include the effect of magnetic non-linearity. This model is used to predict the drive performance at steady state and in the dynamics. The optimal control parameters are obtained by using the dynamic model. A linear model of the converter is used in the dynamic model. The semiconductor switch and diode parameters used in the dynamic model, are obtained from the manufacturer's provided data. The core loss model presented in [15] is used with the SRM non-linear model to predict the core losses of each designed SRMs.

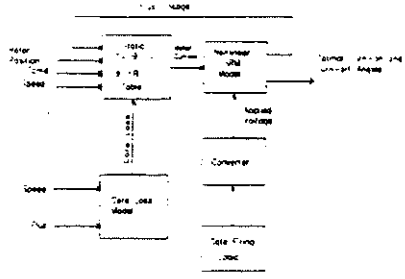

Fig. 1. A Block Diagram of the Dynamic SRM Model

IV. DETERMINATION OF THE OPTIMAL CONTROL PARAMETERS

Base speed in any motor is defined as the speed at which the back emf equals the bus voltage. Motor also reaches its rated power at this speed for rated excitation (current). Torque in SRM below base speed, when the back emf is lower than the bus voltage is controlled, like all other motors, by the PWM control of current. Above base speed, due to the high back emf which can not be field weakened, PWM control of current is not possible. Operation in constant power is made possible in this motor by the phase advancing of the stator phase current until overlapping between the successive phases occurs [9]. Torque control below base speed can be optimized by the stator current profiling [10,11]. However, above base speed the only control parameters are the phase turn-on and the turn-off angles. The phase turn-on and the turn-off angles can be optimally controlled above base speed to maximize the range of the constant power operation with maximum torque per ampere. To find the optimal turn-on and the turn-off angles, the dynamic model developed in the earlier section is used. The search procedure for the optimal angles is lengthy and time consuming. Any standard root seeking methods, such as the Secant method [12], may be used to accelerate the speed of the searching process. After series of iterations, the dynamic model finds the optimal turn-on and turn-off angles. To implement the control scheme in real time, a Neural Network based controller may be implemented [10].

V. DESIGN METHODOLOGY

The design process starts with the hand calculation of several SRM geometries with varying pole numbers and pole dimensions. A 2-D finite element analysis is then performed to obtain the nonlinear field solutions within the motor. The finite element field solutions are used in the development of a nonlinear SRM model. The developed model is used to search the optimal control parameters which extends the constant power range of each motor with maximum torque per ampere. The steady state and the dynamic performances of each designed SRM are investigated for these optimal control parameters. These steps are repeated for each designed SRM in an attempt to determine an appropriate

SRM geometry for EV and HEV applications. In this paper, we will consider only the 8-6 and 6-4 SRM geometries. SRM geometries with more stator and rotor poles will have less space for phase advancing. As a consequence, motor will suffer from limited constant power range. Moreover, the ratio of the aligned to un-aligned inductance will reduce with increased number of rotor and stator poles. This will reduce the static torque and increase the converter volt-ampere [9].

VI. Design Examples

In this section we will present several SRM designs and will investigate their performances when controlled optimally. Our goal is to extend the constant power range with maximum torque per ampere. Special attention will also be given on the drive efficiency. All the design examples considered in this paper have almost the same stator outer dimension and stack length. We begin with the 6-4 SRM designs.

A. 6-4 SRM Design

First we will examine the effect of the pole widths on the SRM performances. The minimum stator and rotor pole widths of a 6-4 SRM should be 30° in order to have adequate starting torque from all positions. To maximize the room available for winding placement, we will keep the stator pole width fixed at 30° and while the rotor pole widths will be varied. The considered SRMs have the following dimensions

- Stator outer diameter, 13.58 inch.
- Rotor outer diameter, 7.4694 inch.
- Stack length, 7.4694 inch.
- Air gap, 0.0373 inch.
- Stator slot height, 1.7166 inch.
- Rotor slot height, 0.9763 inch.
- Stator core thickness, 1.3017 inch.
- Rotor core thickness, 1.3517 inch.
- M19 steel.
- Shaft diameter, 2.8135 inch.
- Number of turns per pole, 14.
- DC bus voltage, 240 V.
- Rated phase current, 168.3 ampere (Air cooled, 4 A/mm^2).
- Stator pole arc, 30°.
- Rotor pole arcs, 30.31° (same pole width as the stator), 31.5°, 34°, and 36°.

The dimensions of the four SRMs are same except for the rotor pole arc, which varies from 30.31° (same as the stator pole width) to 36°. For convenience, we will label these designs as design 1 through design 4. Finite element analysis is performed on each of these motors in order to obtain the nonlinear field solutions. These field solutions are then used in the nonlinear model to determine the steady state and the dynamic performances of each designed SRMs. Fig. 2(a) shows the constant power ranges of these motors. The optimal turn on and the turn off angles and the phase rms currents for the constant power operation of Fig. 2(a) are shown in Fig. 2(b). An extended speed constant power

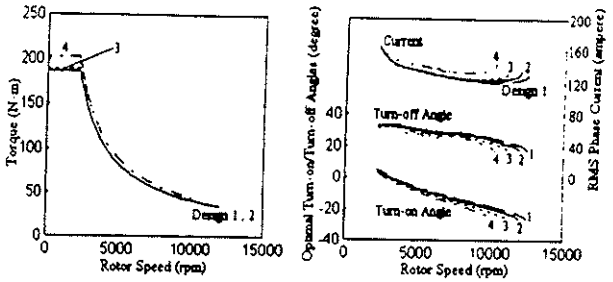

Fig. 2. Extended constant power range (a) and optimal control angles and rms phase current (b) for SRM designs 1-4.

ranges are obtained for these designs when controlled with the optimal parameters. The extended constant power range is maximum (5.7 times the base speed) for design 1 (narrowest rotor pole), while it is minimum (4.7 times the base speed) for design 4 (widest rotor pole). However, the rated torque is minimum for design 1 and maximum for design 4. The long constant power range available from motor 1 will make it highly favorable for vehicle applications, despite the fact that it has a lower rated torque (power). The vehicle performance analysis for all these motors will be presented later. We can see in Fig. 2(b) that lower than rated rms current is needed at higher speeds to maintain constant power at the output. This is a direct consequence of the fact that the power factor (pf) of operation of the motors is improving at higher speed. The power factors and the drive efficiencies for theses motors are presented in Fig. 3 for the constant power operation. We have used the following definition for calculating the pf.

$$\text{pf} = \frac{\text{Output Shaft Power}}{\text{Input RMS VoltAmpere}} \qquad (1)$$

Design 1 exhibit both the best efficiency and the pf among these designs.

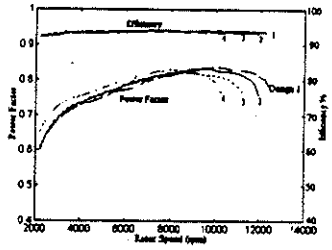

Fig. 3. Efficiency and pf of motors 1-4 for constant power operation.

Since the rms phase current decreases during high speed constant power operation, it should be possible to obtain more than the designed rated powers from these motors at high speed without exceeding the bus voltage and the rated current of each motors. This is shown in Fig. 4. Fig. 4(a) shows the maximum power available from these motors and 4(b) shows the phase current and the control angles for

the maximum power outputs. The output shaft powers are shown as a ratio of the ideal output power (unity pf) which is only possible from a separately excited dc motor. The power curves shown in Fig. 4 are the maximum powers these motors are capable of delivering, given the voltage and the

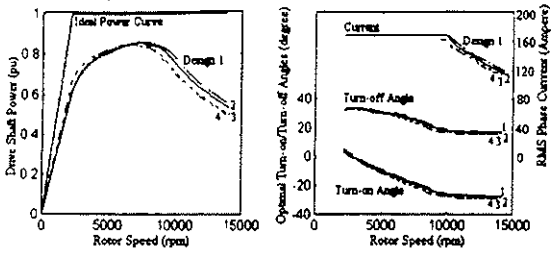

(a) (b)

Fig. 4. Maximum output power (a) and optimal control angles and rms phase current (b) for SRM designs 1-4.

current limitations. Again, design 1 is exhibiting better performance (higher power) at higher speeds. It may be noted that almost 40% more than the design rated power is obtained. The difference between the ideal power and the actual power is narrowing at the high speed. It is interesting to note that, beyond a certain speed the rms phase current is reduced from the rated value in order to obtain more power. Any current higher than this will actually reduce the output torque due to the development of more negative torque. Hence, beyond that speed it is advantageous to reduce the current rather than maintaining the rated current. Motor efficiency and power factor for its operation on the maximum power curve of Fig. 4(a) are shown in Fig. 5. Although the rated pf is low for SRM, this difficulty is greatly overcome at higher speeds and the SRM output power approaches the ideal power (Fig. 4). This will make SRM attractive for applications requiring high speed operations, *e.g.*, the vehicle propulsion system.

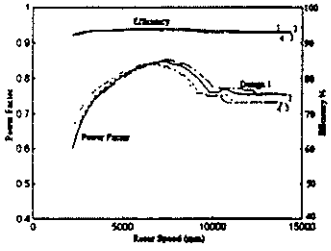

Fig. 5. Efficiency and pf of motors 1-4 for maximum power output.

Vehicle application also requires short term overload capability from its propulsion system. Hence, finally, we will examine the overload capabilities of these motors. SRM does not have any break down torque like the induction motor. The overload capability, however, would depend on how much current can be pushed in to the motor against the high back emf and how fast it can be pushed. Obviously, a low unaligned inductance will be favorable for both these conditions. Design 1 which has narrow poles (low unaligned inductance) will have like it's extended power capability a good overload capability. This is shown in Fig. 6 in pu of the rated power. As expected, maximum overload capability decreases as the speed increases. Peak overload capability for design 1 at the rated speed is almost 4.5 times its rated

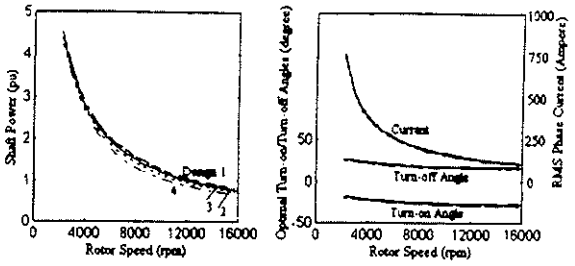

(a) (b)

Fig. 6. Maximum overload power (a) and rms phase current and optimal angles (b) for SRM designs 1-4.

power. RMS phase current and optimal control angles are shown in Fig. 6(b). These phase currents for the overload condition may be compared with the currents of Figs. 2 and 4, to understand the extent of overload from thermal (cooling requirement) point of view. We would, however, like to point out that the actual overload power would be less than this theoretically predicted overload power. When the motor is severely overloaded, the back iron will saturate. This will introduce strong coupling between phases, which is neglected in the developed model of this paper. Due to this phase couplings, torque and hence power will be reduced. Efficiency and pf during motor overloading are shown in Fig. 7.

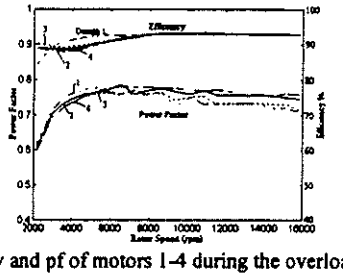

Fig. 7. Efficiency and pf of motors 1-4 during the overloading condition.

Next, we will investigate the effect of rotor pole height on the SRM performance. If the stator outer diameter is fixed, an increase in rotor pole height, however, will decrease the stator slot area. As a consequence, winding area will decrease. Hence, the rated current of the motor will decrease. In the unaligned position, flux also fringes through the side of the rotor pole. Hence, making the rotor pole very long will not be very useful in reducing the unaligned inductance. We will consider four more designs. The rotor pole height of design 2 (rotor pole arc 31.5°) is increased 10% and 20%, these two designs will be labeled design 5 and design 6 respectively. Also, the rotor pole height of design 3 (rotor pole arc 34°) is increased 10% and 20%. These two designs will be labeled design 7 and design 8 respectively.

As before, the finite element analysis is performed on these motors to obtain the field solutions. The non-linear field solutions are then used in the non-linear SRM model to examine the drive performance. For better understanding, the

performance of designs 5-8 will be presented along with the performance of design 2 and 3. Fig. 8 shows the constant power ranges of these motors when controlled optimally. Design 6, which has the narrowest and longest rotor poles

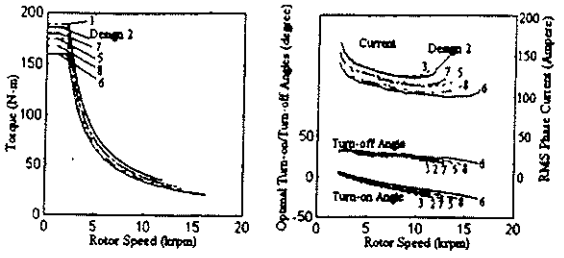

(a) (b)

Fig. 8. Extended constant power range (a) and optimal control angles and rms phase current (b) for SRM designs 5-8.

among these designs, has the longest constant power range (7.75 times the base speed!), however, the lowest rated torque. On the other hand, design 3, which has the widest and shortest rotor pole, has the highest rated torque but the shortest constant power range (5.1 times the base speed). The pf and the efficiency of these designs for the constant power operation are shown in Fig. 9.

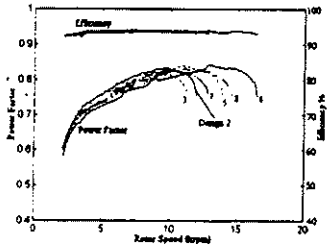

Fig. 9. Efficiency and pf of motors for constant power operation.

The maximum power available from these motors, operating within the voltage and the current limitations, is shown in Fig. 10 and the corresponding efficiencies and power factors are shown in Fig. 11. The overload capabilities of these motors are shown in Fig. 12 and the power factors and the efficiencies are shown in Fig. 13. Design 6 has an overloading capability of almost seven times the rated power.

Among the 8 designs we have presented so far, design 6 has the longest constant power range, however, the lowest power rating, while design 4 has the shortest constant power range, however, the highest power rating. A valid comparison between these motors, however, should be made in terms of the vehicle performances, which we will make in the next section. We will present two 8-6 SRM designs next.

B. 8-6 SRM Design

We will present two 8-6 SRM designs in this sub-section. These two designs have the following dimensions

- Stator outer diameter, 13.66 inch.
- Rotor outer diameter, 7.5156 inch.
- Stack length, 7.5156 inch.
- Air gap, 0.0376 inch.
- Stator slot height, 1.9303 inch.
- Rotor slot height, 1.3152 inch.
- Stator core thickness, 1.1066 inch.
- Rotor core thickness, 1.1987 inch.
- M19 steel.
- Shaft diameter, 2.4878 inch.
- Number of turns per pole, 11.
- DC bus voltage, 240 V.
- Current density 4 A/mm^2 (Air cooled).
- Stator and rotor pole arcs 21°, 23° (Design 9), and 19°, 21° (Design 10).

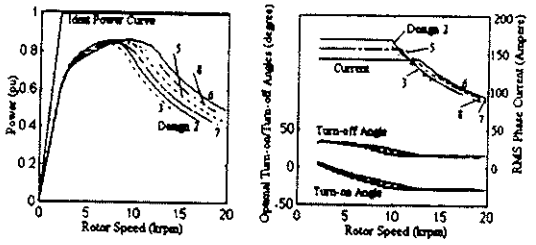

(a) (b)

Fig. 10. Maximum output power (a) and optimal control angles and rms phase current (b) for SRM designs 5-8.

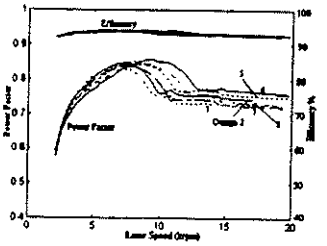

Fig. 11. Efficiency and pf of motors 5-8 for maximum power output.

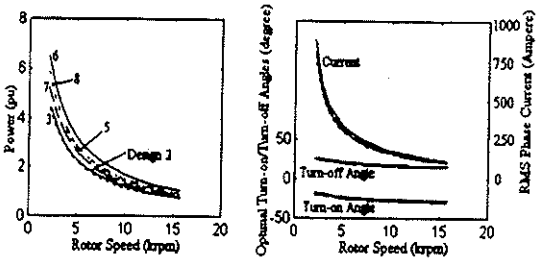

(a) (b)

Fig. 12. Maximum overload power (a) and rms phase current and optimal angles (b) for SRM designs 5-8.

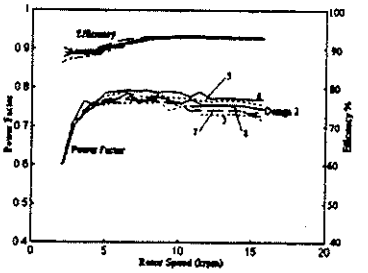

Fig. 13. Efficiency and pf of motors 5-8 during the overloading condition.

We have labeled the two SRM designs presented in this sub-section as design 9 and design 10. After performing the finite element analysis, the optimal constant power ranges are

calculated using the dynamic model. Fig. 14 shows the constant power ranges of these motors along with the rms phase current and the optimal angles. Design 9 which has wider poles produces higher rated torque, however, a constant power range of only 3.2 times the base speed. Design 10 has slightly lower rated torque and rated power than design 9, but has a much longer constant power range (4.125) than 9. The rms phase current also decreases while maintaining the constant power operation. The power factor and motor efficiency for the constant power operation are shown in Fig. 15. Power factor improves considerably in the

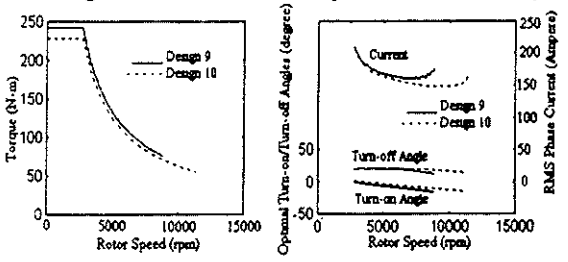

(a) (b)

Fig. 14. Extended constant power range (a) and optimal control angles and rms phase current (b) for 8-6 SRM designs 9 and 10.

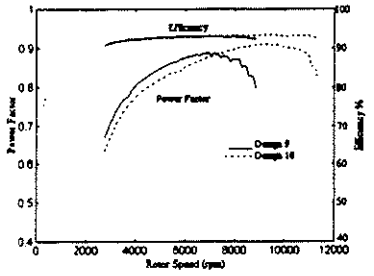

Fig. 15. Efficiency and pf of operation for motors 9 and 10 for their operation on the constant power profile.

high speed constant power operation of the motors. Design 10 has a lower power factor than design 9 at the rated speed, however, improves rapidly and shows better power factor than design 9 roughly after 7000 rpm. The 8-6 designs, although have shorter constant power range, are showing better power factor and much better power ratings than the 6-4 designs (Fig. 2,3). The 8-6 SRMs, due to their narrower pole widths than the 6-4 SRMs, operate in higher saturation level (6-4 and the 8-6 designs have comparable winding areas). Moreover, the higher phase overlapping in 8-6 motors are contributing more to the average torque. The back iron in 8-6 designs are, however, saturating. The stator and rotor back iron thickness in both the design are chosen 80% of the design 9 respective pole widths. The back irons in both the design, especially in the design 10 (design 10 has higher ampere-turn rating), saturate for the rated torque and near the rated speed of the motor. To prevent this from happening, design 9 would require 6% more core thickness, whereas design 10 would require 20% more core thickness.

Next, we will examine the maximum power capability operating within the rated voltage and current of the motors. Fig. 16 shows the maximum power capability of these two motors in per unit of their ideal output power. Design 10 has higher and wider power capability at high speeds. This is obviously desirable for EV and HEV applications. Efficiency and power factor for this operation are shown in Fig. 17. Design 10 i also showing higher power factor and efficiency at higher speeds.

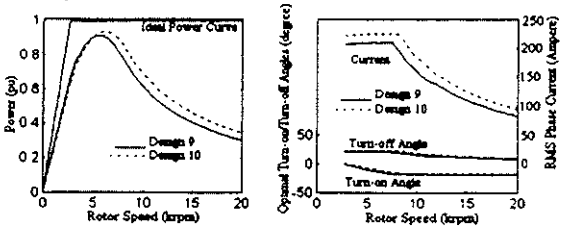

(a) (b)

Fig. 16. Maximum output power (a) and optimal control angles and rms phase current (b) for SRM designs 9 and 10.

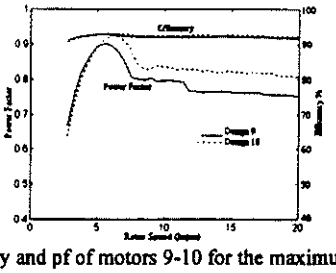

Fig. 17. Efficiency and pf of motors 9-10 for the maximum power output.

Finally, in Fig. 18 we show the overload capabilities of these designs. The power factors and efficiencies for the overloaded operation are shown in Fig. 19. Design 10 has better pf, better efficiency, and also better overload capability. Due to the higher unaligned inductance, the overload capability of the 8-6 designs are, however, lower than the 6-4 designs.

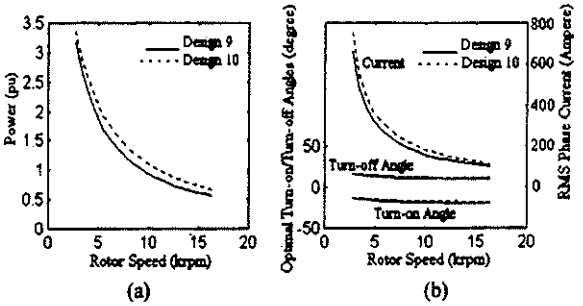

(a) (b)

Fig. 18. Maximum overload power (a) and rms phase current and optimal angles (b) for SRM designs 9 and 10.

In this section, we have presented eight 6-4 SRM designs and two 8-6 SRM designs. The 6-4 designs are showing much longer constant power capability and much higher overload capability than the 8-6 designs. The 8-6 designs, however, have higher rated torque and power. They also exhibit better power factor and efficiency. A valid comparison between these designs can only be made if we compare the vehicle performances, *e.g.* the initial acceleration performance, when these motors are used as the

propulsion system. This comparison will be made in the next section.

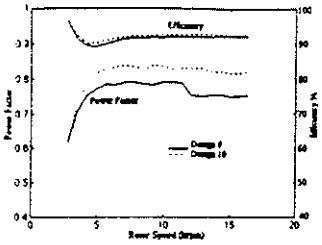

Fig. 19. Efficiency and pf of motors 9 and 10 during overloading condition.

VII. Vehicle Performance Analysis

In this section, we will compare the performances of the designed SRMS for a vehicle propulsion system by calculating the 0-60 mph acceleration time. The SRM performance will also be compared with the performances of induction motor (IM) and brushless dc (BLDC) motor. For the later comparison, we will calculate the power and the input volt-ampere requirements of IM and BLDC motor for the 0 to 60 mph acceleration in times specified by the SRMs. For this purpose, we consider the following vehicle

- vehicle rated speed of 26.82 m/s (60 mi/h);
- vehicle maximum speed of 44.7 m/s (100 mi/h);
- vehicle mass of 1450 kg;
- rolling resistance coefficient of 0.013;
- aerodynamic drag coefficient of 0.29;
- frontal area of 2.13 m^2;
- wheel radius of 0.2794 m (11 in);
- level ground
- zero head wind

For calculating the acceleration time, the maximum power capabilities of SRMs, presented in Figs. 4, 10, and 16, will be assumed. For calculating IM power and volt-ampere we will assume a constant power capability of 4 times the base speed and a pf of 0.8. While, a constant power range of 2.2 times the base speed and a pf of 0.9 will be assumed for BLDC motor.

Table I is listing the 0-60 mph acceleration time, power, and input KVA ratings of the IM, BLDC motor, and SRMs.

Table I
Motor power ratings and vehicle acceleration time

SRM Design #	Accl. time (s)	SRM Power (kW)	SRM KVA	IM Power (KW)	IM KVA	BLDC Power (KW)	BLDC KVA
1	13	42.1	69.8	57.88	72.35	75.5	83.9
2	13.25	42.56	69.86	56.9	71.13	74.43	82.7
3	13.48	42.61	69.9	56	70	73.27	81.41
4	13.58	45.88	69.85	55.68	69.6	72.78	80.86
5	13.85	39.1	64.76	54.7	68.38	71.46	79.4
6	14.78	34.6	59.35	51.68	64.6	67.39	74.88
7	14.1	38.98	64.68	53.85	67.3	70.34	78.15
8	15.01	35.38	59.32	50.1	62.6	66.4	73.77
9	10.1	68.12	101.4	72.7	90.88	95.67	106.3
10	8.74	69.95	109.3	83.04	103.8	109.6	121.8

Among the 6-4 designs, design 1, which has the narrowest rotor poles requires least amount of time for the acceleration. Design 6, which has the longest constant power range, is requiring longer time for the initial acceleration due to its lower power rating. The 8-6 designs have much higher power rating than the 6-4 designs, the acceleration time is therefore much lower for the 8-6 designs, despite their relatively lower constant power range. The 6-4 SRMs have better overload capability than the 8-6 designs. They also operate in a lower level of saturation. Their performance, therefore, can be improved significantly by increasing the current density. However, more efficient cooling of the motor would be required. The rotor pole height of designs 1-4 can also be reduced to make more room for phase windings. This will, however, increase the unaligned inductance and consequently, the constant power range, the overload capability, as well as the pf will be reduced. SRMs are exhibiting equal or better performances than the induction and BLDC motors.

VIII Experimental Result

SRM designs presented in section VI show that an extremely long constant power range is possible if the motor is designed appropriately and controlled optimally. A range of three to seven times the base speed has been demonstrated with different designs. In this section, we will present experimental results to demonstrate that an extended constant power range is possible from SRM. The experimental motor, however, is a small motor available commercially. The motor was not designed specifically following the methodology presented in this paper. However, it will be controlled with the optimal control parameters. The optimal control parameters are calculated from the dynamic model. The nonlinear field solutions for this motor is calculated from the experimentally collected data. Simulation results for this motor show that an extended range exceeding 6.5 times the base speed is possible. A detailed simulations results of this motor can be obtained in our other paper [16].

Fig. 20 shows the experimentally measured torque and rms phase current at high speed when the motor is controlled

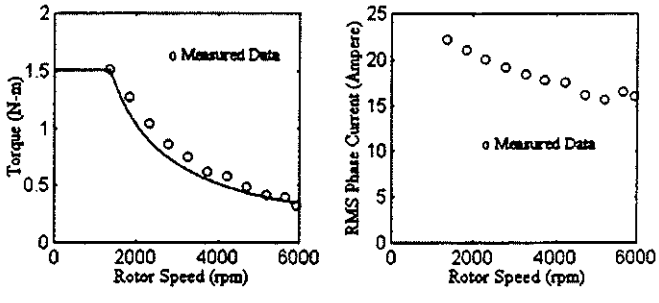

(a) (b)

Fig. 20. Experimentally measured torque (a) and rms phase current (b) at high speed.

optimally. The experimental setup has a maximum speed limitation of 6000 rpm. Therefore, we limited our experiment to 6000 rpm. The measured constant power range is almost 4.35 times the base speed. There is still some room available for phase advancing. This can be seen from the phase current waveform near 6000 rpm (Fig. 21). The measured rms phase current decreases while maintaining constant power, indicating, as predicted theoretically, an improvement in the power factor.

IX. Conclusion

High speed capabilities of several 6-4 and 8-6 designs are presented in this paper. Simulation results are showing some interesting characteristics of the SRM. An extremely long constant power ranges are available from the 6-4 designs. Power factor improves significantly at the high speeds from its low speed values. Almost 40% more than the design rated power is obtained at high speed without exceeding the voltage and the current ratings of the motors. Excellent efficiencies are exhibited by these designs at high speed. The design examples presented in this paper by no means are the best design geometries. Nevertheless, a design methodology is presented and the potential of SRM for vehicle application is clearly demonstrated. SRM definitely shows the potential to perform superior to brushless dc and induction motors. A constant power range of more than four times the base speed is demonstrated by the 8-6 experiment motor. The experimental result also demonstrate the improvement of pf at the high speed operation.

Acknowledgment

The support of Texas Higher Education Coordinating Board Advanced Technology Program, Texas Transportation Institute, and Texas Instrument Digital Control Systems Division, for this research is gratefully acknowledged.

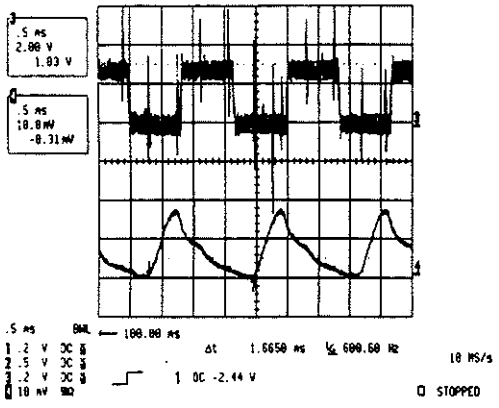

Fig. 21. Actual (the lower trace) and the commanded (the upper trace) current at 6000 rpm. The oscilloscope scales are 21 and 20 amperes per division for the commanded and the actual current respectively.

X. Reference

[1] P. J. Blake, R. M. Davis, W. F. Ray, N. N. Fulton, P. J. Lawrenson, and J. M. Stefenson, "The control of switched reluctance motors for battery electric road vehicles," *International Conference on PEVD*, pp. 361-364, May, 1984.

[2] J. H. Lang and F. J. Vallese, "Variable reluctance motor drives for electric propulsion," *United States Department of Energy Report*, DOE/CS-54209-26, May, 1, 1985.

[3] J. Corda and J. M. Stephenson, "Analytical estimation of the minimum and maximum inductances of a doubly-salient motor," *on Proc. Int. Conf. Stepping Motors Syst. (University of Leeds)*, 1979, pp. 50-59.

[4] T. Uematsu and R. S. Wallace, "Design of a 100 kW switched reluctance motor for electric vehicle propulsion," *APEC*, pp. 411-415, 1995.

[5] M. Ehsani, K. M. Rahman, and H. Toliyat, "Propulsion system design of electric and hybrid vehicles," *IEEE Trans. on Industrial Electronics*, vol. 44, no. 1, February 1997.

[6] J. V. Byrne, and J. B. O'dwyer, "Saturable variable reluctance machine simulation using exponential functions," *Proceedings of the International conference on Stepping Motors and Systems*, University of Leeds, UK, 1976, pp. 11-16.

[7] T. J. E. Miller and M, McGlip, "Nonlinear theory of switched reluctance motor for rapid computer-aided design," *IEE Proceedings*, vol. 137, Pt. B, No. 6, pp. 337-347, Nov. 1990.

[8] D. A. Torrey, X.-M. Niu, and E. J. Unkauf, "Analytical modeling of variable-reluctance machine magnetization characteristics," *IEE Proc. Electr. Power Appl.*, vol. 142, no. 1, pp. 14-22, Jan. 1995.

[9] T. J. E. Miller, "Switched reluctance motor and their control," Clarendon Press, 1993.

[10] K. M. Rahman, A. V. Rajarathnam, and M. Ehsani, "Optimized instantaneous torque control of switched reluctance motor by neural network," *IEEE IAS Conference Record*, New Orleans, Oct. 1997.

[11] I. Husain, K. R. Ramani, and M. Ehsani, "Torque ripple minimization in switched reluctance motor drives by PWM current control," *IEEE Trans. on Power Electronics*, vol. 11, no. 1, pp. 83-88, January, 1996.

[12] A. Ralston and P. Rabinowitz, *A First Course in Numerical Analysis*, 2nd ed. New York: McGraw-Hill, 1978.

[13] T. J. E. Miller, *Brushless Permanent-Magnet and Reluctance Motor Drives*, Oxford Science Publication, Oxford, 1989.

[14] W. L. Soong and T. J. E. Miller, "Field weakening performance of brushless synchronous AC motor drives," *IEE Proc.-Electr. Power Appl.*, Vol. 141, No. 6, pp. 331-340, November 1994.

[15] P. N. Materu and R. Krishnan, "Estimation of Switched Reluctance Motor Losses," *IEEE Trans. on Industry Applications*, Vol. 28, No. 3, pp. 668-679.

[16] K. M. Rahman, G. Suresh, B. Fahimi, A. V. Rajarathnam, and M. Ehsani, "Optimized torque control of switched reluctance motor at all operational regimes using neural network," *IEEE IAS Annual Meeting*, St. Louis, 1998.

970294

Parametric Design of the Drive Train of an Electrically Peaking Hybrid (ELPH) Vehicle

Yimin Gao[1], Khwaja M. Rahman, and Mehrdad Ehsani
Texas A&M Univ.

ABSTRACT

The operation of an electrically peaking hybrid vehicle (ELPH) can be divided into two basic modes. • Constant or cruising speed mode in which a small internal combustion engine (ICE) is used to power the vehicle. • Peak power mode in which the combination of an electric motor and ICE is used to supply peak power for acceleration and limited-duration steep hill climbing of the vehicle.

A method, by which the engine size and the speed reduction ratio from the engine to drivewheels can be developed based on the cruising mode, is presented in this paper. The electric motor power rating and the motor gear ratio to the drive wheels can then be determined, based on the acceleration and gradeability. The results show that a simple single-gear transmission would be a good selection for overall performance.

INTRODUCTION

Petroleum fueled, internal combustion engine powered vehicles are the most popular means of transportation, because of their high energy density and relatively high power density. However, in recent years, increasing concern over air pollution, caused by tailpipe emissions of the petroleum-based vehicles, and the dwindling petroleum resources have caused the automotive engineers and automakers to re-evaluate the designs of the conventional internal combustion engine powered vehicles. The conventional automotive drive train suffers from a number of disadvantages :

1. The inherently mismatched speed-torque characteristic of the engine and the vehicle necessitates a complicated transmission, with its associated losses and inflexibility.

2. In order to have ample power for acceleration and gradeability with a limited number of transmission gears, the engine must be oversized to roughly ten times that required for cruising at *100 Km/h* on a level road and three or four times that required for maintaining *100Km/h* on a *6%* grade.[1]

3. Today's internal combustion engines show a significant difference in specific fuel consumption between partial load and the optimal operating point, which is close to full load as shown in *Fig. 1*. An oversized engine moves the cruising operating point away from the optimal operation point. Consequently, ICE vehicles have low efficiency [2].

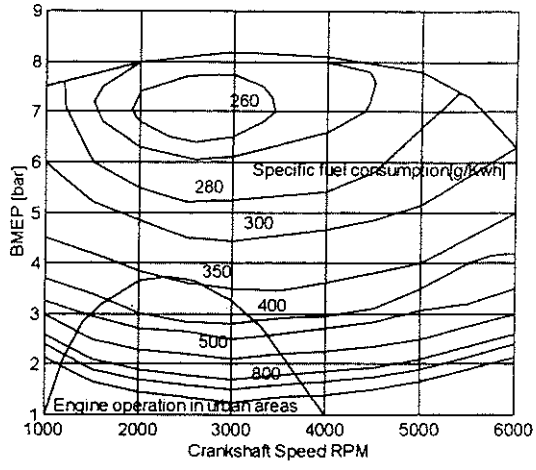

Fig. 1. Typical SI-engine SFC Map with Actual Operation Point[2]

The electric motor, in addition to its clean, quiet and efficient operation, has inherent flexibility in its speed-torque control. *Fig. 2* shows a typical torque-speed characteristics of the electric motor with power electronic drive. The motor can operate anywhere within this torque-speed boundary. This

[1] Visiting scholar from Jilin University of Technology, China

allows the motor to meet the vehicle torque-speed requirements at all times, without a variable gear transmission. However, pure electric vehicles (Ev's) suffer from other disadvantages[9].

1. The heavy and bulky battery pack, with its relatively small energy storage, makes the EV limited in range, and load carrying capacity.

2. Long charging time limits the EV's practicality.

Therefore, commercial success of the EV depends strongly on the development of advanced batteries. However, progress in batteries over the past several decades has not been adequate.

The hybrid configurations, in which two power sources are applied to propel the vehicle, show significant promise[7,8]. The hybrid electric-internal combustion engine drive train, if properly configured, can combine many of the advantages of both EV and ICE vehicles [9].

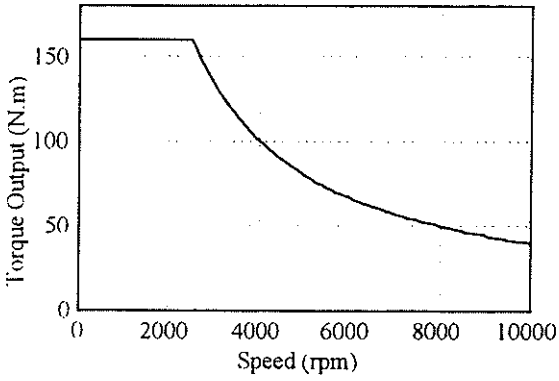

Fig. 2. The Speed-torque Characteristic of Electric Motor

ELECTRICALLY PEAKING HYBRID CONFIGURATION

The operation of passenger vehicles can be divided into two basic modes: constant speed (cruising), and acceleration (peak power). In cruising mode, relatively low power is required from the drive train. However, large amount of energy is consumed in a long trip. In acceleration mode, high peak power is required but not much energy is consumed, due to its brief and transient occurrence. Proper parallel combination of ICE, for cruising operation, and electric motor with a small battery pack, for acceleration, can satisfy these requirements in a viable drive train. The motor with a small chemical battery pack optimized for high power would have acceptable power capability and power density for acceleration[3]. A small ICE with a small fuel tank would have the energy density for cruising and recharging the battery for the next acceleration.

A configuration of such an electrically peaking hybrid (ELPH) vehicle is shown in *Fig. 3* in which the base power unit is the engine and peaking power unit (or load leveling device) is the electric motor.

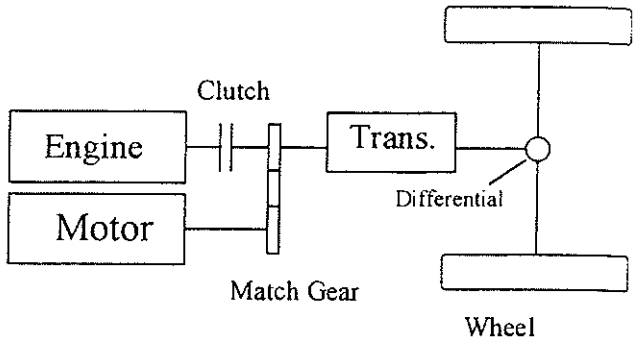

Fig. 3 The Configuration of an Electrically Peaking Hybrid (ELPH) Vehicle

The ELPH configuration, in addition to satisfying the requirements of acceleration and gradeability, has the ability to recover braking energy with the electric motor functioning in regenerating mode. Furthermore, when the vehicle operates with light load, such as at a low constant cruising speed or going down a slight hill, the engine can recharge the battery pack to maintain adequate state-of-charge. More beneficially, this enhances the engine load, for operation close to its optimal point. A well designed ELPH vehicle may never use an external source to charge its battery pack and can achieve an excellent fuel economy.

In this paper, the following specification of the Electrically Peaking Hybrid (ELPH) vehicle prototype, which is being developed at Texas A&M University, will be taken as the example.

Curb weight	*1700 kg,*
Rolling resistance coefficient of tire	*0.013,*
Aero-dynamic drag coefficient	*0.29,*
Front area	*2.13 m^2,*
Wheel radius	*0.2794 m.*

CRUISING MODE

As described above, when the vehicle operates on level ground with a constant cruising speed, the engine alone delivers power to the drivewheels. Consequently, the performance of the vehicle is determined only by the engine power and speed reduction ratio from the engine to the drivewheels.

ENGINE POWER REQUIREMENT- The determination of the engine power plays a very important role in the design of ELPH vehicle. An oversized engine would lose its fuel-saving advantage as in the conventional vehicles. On the other hand, an undersized engine can not deliver enough power to meet the requirements of the vehicle. Therefore, a large battery pack and a large motor would be needed to compensate for the shortage of engine power. Consequently, the ELPH vehicle would suffer from the same problems as an EV.

When the vehicle operates on a level ground with a constant cruising speed, the engine must deliver enough power to overcome the vehicle load power which includes the rolling resistance power and the aero-dynamic drag power. Thus, the required engine power output is

$$Pe = \frac{v}{1000\eta_{et}}\left(mgf + \frac{1}{2}\rho C_D A v^2\right) \qquad (1)$$

where, v = speed of vehicle, *m/s*,
η_{et} = efficiency of the transmission form engine to drivewheels, *0.9*
m = vehicle mass, *Kg*,
f = rolling resistance coefficient,
g = gravity acceleration, *9.81 m/s²*,
C_D = aero-dynamic drag coefficient,
A = front area of the vehicle, m^2,
ρ = air density, *1.228 Kg/m³*.

Fig. 4. shows the vehicle load power as a function of the vehicle speed in cruising mode This figure indicates that not much power is needed to maintain the vehicle operation in cruising mode. About *30 Kw* of power capacity will be plenty to meet the requirement of the vehicle at a speed of *130 Km/h (81.5 mph)*. This *30 Kw* of engine power capacity is quite small in comparison to the average *50* to *70 Kw/1000Kg* specific power of conventional cars More precise selection of the engine power capacity will be made with consideration of recharging of the peaking battery pack

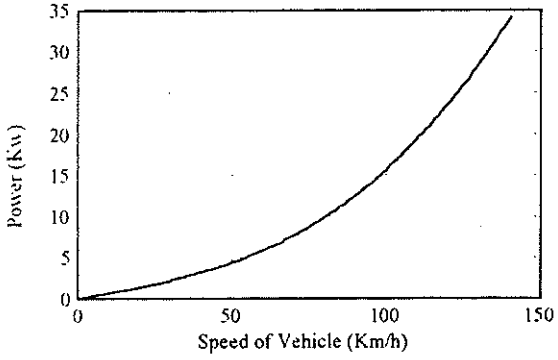

Fig. 4. Required Engine Power Versus Constant Speed on A Level Road

DIFFERENTIAL GEAR RATIO-*Fig. 5.* shows the speed-power characteristics of a typical gasoline SI engine. Equation (2) gives the vehicle speed for a single-gear transmission or a top gear operation of a multi-gear transmission. By equation (2), *Fig. 5* can be transformed into a vehicle speed-power profile, as shown in *Fig. 6.*

$$v = \frac{\pi r N}{30 r_d} \quad (m/s) \qquad (2)$$

where, r_d = differential gear ratio drivewheels,
r = radius of the drivewheel, *m*
N = speed of engine, *rpm.*

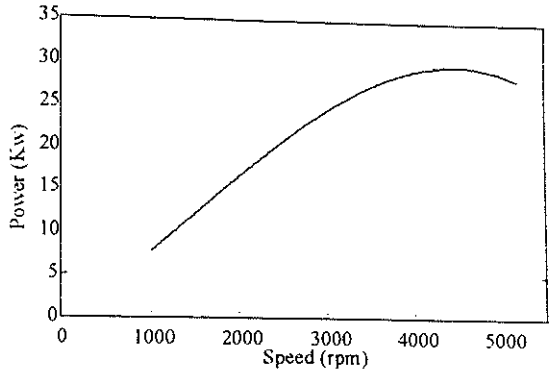

Fig. 5. Typical Characteristics of SI Engine

In *Fig. 6.* several engine power curves with different differential gear ratios are shown along with the vehicle resistance power curve. The top speeds of the vehicle with different differential gear ratios are represented by the crossing points of engine power curves with resistance curve (such as v_{2max}, v_{3amx} and v_{4max} corresponding to r_{d2} , r_{d3}, and r_{d4}) or by the maximum rpm of the engine (such as v_{1max} corresponding to r_{d1}). *Fig. 6* indicates that, with r_{d3}, the vehicle has a highest top speed which corresponds to the peak power of the engine. However, with r_{d2}, the vehicle has more remaining power, defined as the difference between the engine power curve and vehicle resistance power curve only a slight top speed reduction. The remaining power can be used for acceleration or grade climbing or battery charging . As shown in *Fig. 6*, with a gear ratio of r_{d2} and at a speed of *100 Km/h*, the engine has about half of its power remaining. A large gear ratio, such as r_{d1}, will allow the vehicle to have more remaining, but the top speed will suffer a significant reduction. In contrast, too small a gear ratio, such as r_{d4}, will allow the vehicle to have a small remaining power. For a small engine with the addition of battery charging load, the differential gear ratio of r_{d2} is a suitable selection.

ACCELERATION MODE

When the vehicle experiences acceleration or steep hill climbing, high traction peak power is needed. This high transient power (peaking power) is supplied by both the engine and the motor working together. In the ELPH vehicle, the contribution of the electric motor drive to the peak power should be dominant. Thus, the acceleration and maximum gradeability of the ELPH drive train is mainly determined by the electric motor drive and battery power rating.

ACCELERATION-The ideal characteristic of a power unit for vehicular application is constant power output over the full speed range[4,5,6,]. A vehicle with this kind of power unit does not require a multi-gear transmission to enhance its acceleration and gradeability performance. A well controlled electric motor has speed-torque characteristics that are close

to this ideal, as shown in *Fig. 2*. Here the motor has a constant power output over a large range of speed and a constant torque output over the low speed range. Therefore, the acceleration performance of the ELPH vehicle will be determined by the power rating of the electric motor and is only slightly influenced by the gear number and gear ratios of the transmission.

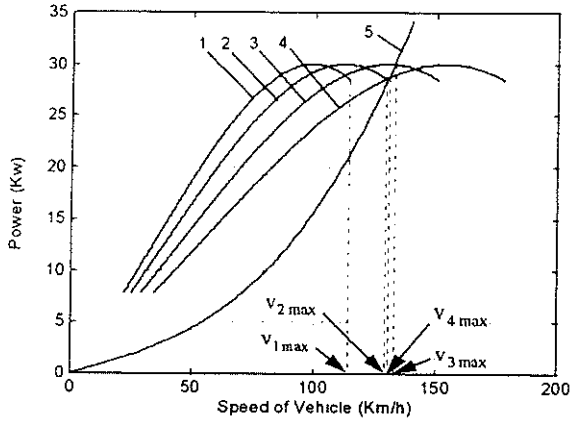

1---r_{d1}=4.78, 2---r_{d2}=4.22,
3---r_{d3}=3.64, 4---r_{d4}=3.08
5--- vehicle resistance power

Fig. 6. Engine Power Output And Resistance Power Versus Vehicle Speed with Different Differential Gear Ratios

The vehicular acceleration on a level ground can be expressed as:

$$\frac{dv}{dt} = \frac{F_t - F_w - F_f}{\delta m} \quad (m/s^2) \qquad (3)$$

where, $F_t = (T_e + T_m r_m) r_t r_d \eta_t / r$, the thrust force of ground acting on the drivewheels (T_e and T_m are engine torque and motor torque respectively; r_t and r_d are the transmission and differential gear ratios, respectively; r_m is gear ratio from motor to driveshaft.). $F_w = 0.5\rho C_D A v^2$, the aero-dynamic drug, and $F_f = mgf$, the rolling resistance. δ is the rotational inertia coefficient.

The accelerating time from zero to a desired speed , v^*, can be expressed as:

$$t = \int_0^{v^*} \left(\frac{dt}{dv}\right) dv = \int_0^{v^*} \frac{\delta m}{F_t - F_w - F_f} dv \qquad (4)$$

The calculation of the vehicle acceleration time is somewhat difficult due to the speed-torque characteristic of the engine which, generally, can not be expressed by an explicit formula. However, it may be completed by numerical methods with a computer.

Fig. 7 shows a plots of acceleration times from zero to *96 Km/h* vs. electric motor power with different gear ratios from the motor to the driveshaft, r_m. The assumptions are a *30 Kw* engine, motor characteristics as shown in *Fig. 2*, a differential gear ratio of r_d = *4.23* and transmission gear ratio of r_t = *1.0*.

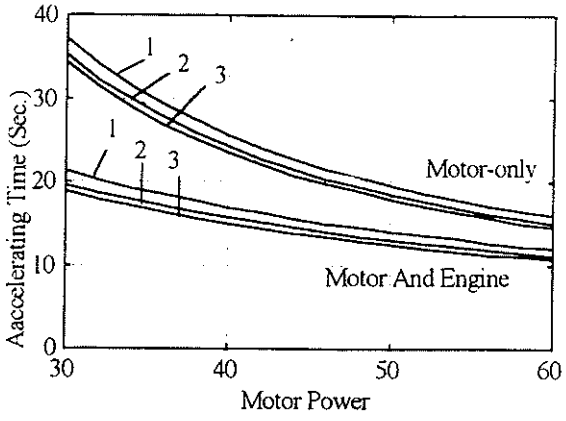

1---r_m=1.5, 2---r_m=1.9, 3---r_m=2.3

Fig. 7. The Accelerating Time Versus Electric Motor Power

As we expected, the gear ratio from the motor to the driveshaft has a small influence on the acceleration time and, the electric motor power plays a dominant role in the acceleration of the vehicle.

Using a computer program, the acceleration time of the vehicle with a multi-gear transmission can also be calculated, as shown in *Fig. 8*. The results indicate that the number of gears in the transmission has a small influence on the acceleration of the vehicle when the differential gear ratio is greater than *4*. This result is desirable because a single-gear transmission can greatly simplify the drive train and the control system.

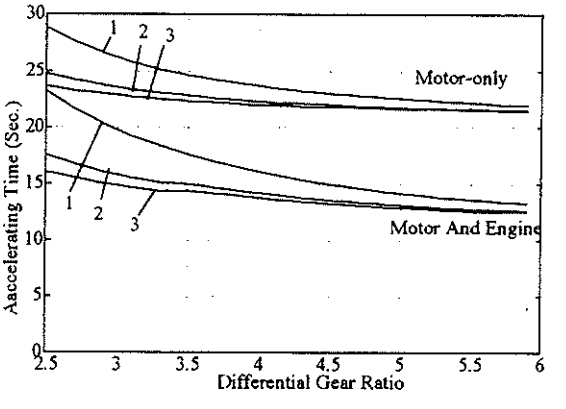

1- gear transmission, gear ratio, 1
2--2-gear transmission , gear ratios , 1.6, 1
3--3-gear transmission , gear ratios, 2.54, 1.6 and 1
Engine power = 30 Kw,
Electric motor power = 42 Kw
Gear ratio from motor to driveshaft, r_m=1.7

Fig. 8. Accelerating Time with Different Number of Gears and Different Differential Gear Ratios

GRADEABILITY-The gradeability of the vehicle is determined by the maximum thrust forces acting on the drivewheels. The gradeability of a vehicle can be expressed by

$$\sin\alpha = \frac{F_t - F_w - F_f}{mg} \qquad (5)$$

where α is the road angle in degrees .

Due to the small aero-dynamic drag at low speeds, the gradeability of the vehicle is mostly determined by the maximum torque of the motor and the engine as well as the gear ratios of the transmission. *Fig. 9* shows the gradeability of the vehicle with a three-gear transmission in which the parameters used are the same as in *Fig. 8*. *Fig. 9* indicates that the gradeability will be greatly enhanced by using a multi-gear transmission. However, in real applications, the vehicle would seldom use the first or second gear for climbing a grade, because, normally, such large grades are seldom encountered in highway and urban driving. This also means that a single-gear transmission would serve the gradeability well.

Fig. 10 shows gradeability versus different power outputs with a single-gear transmission in which the parameters are the same as in *Fig. 8*. Actually, the gradeability can be enhanced, without a need for increasing the gear ratio or applying a multi-gear transmission, by decreasing the base speed of the electric motor. This is accomplished in the low speed, constant torque region of the motor operation

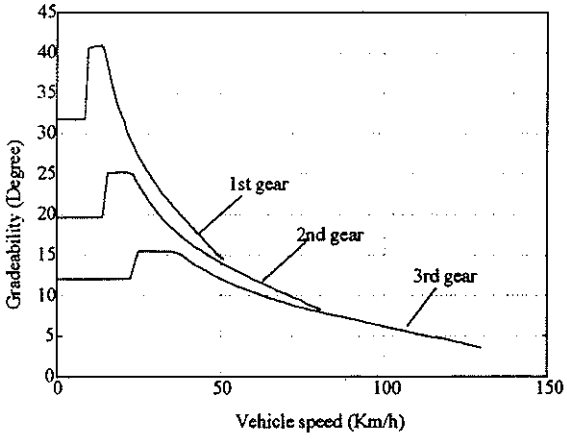

Fig. 9. Gradeability with A Multi-gear Transmission

CONCLUSION

The ELPH vehicle can combine many advantages of conventional and electric vehicles. A well designed ELPH vehicle would have a comparable performance to the conventional vehicle and excellent fuel economy and emission characteristics.

Using the method presented in this paper, the power capacity of a small internal combustion engine and a single speed reduction gear can be used to achieve a satisfactory performance and a excellent fuel economy at cruising speed. Properly selected electric motor power and speed reduction gear can eliminate application of the complicated multi-gear transmission with satisfactory acceleration and hill climbing performance.

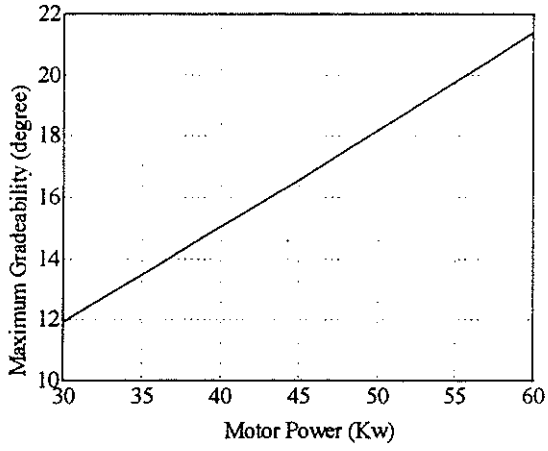

Fig. 10. Gradeability of the Vehicle with Different Motor Power Output And A Single-gear Transmission

ACKNOWLEDGMENT

The financial support of Texas Higher Education Coordinating Board and Texas Transportation Institute for the ELPH project is gratefully acknowledged.

REFERENCE

[1] Timothy C. More and Armory B. Loind, *Vehicle Design Strategies to Meet and Exceed PNGV Goals*, SAE 951906.

[2] Martin Endar and Philipp Dietrich, *Duty Cycle Operation as a Possibility to Enhance the Fuel Economy of an SI Engine at Part Load*, SAE 960229.

[3] A.F. Burke, *Battery Availability for Near Term (1998) Electric Vehicle*, SAE 911914.

[4] J.Y. Wong , *The Theory of Ground Vehicle* , John Wiley & Sons Inc. Press, 1978.

[5] M.Ehsani, K. M. Rahman, and H. Toliyat, *Propulsion System Design of Electric & Hybrid Vehicle*, accepted for publication in the IEEE Tran. on Industrial Electronics.

[6] H.A. Toliyat, K. M. Rahman, and M. Ehsani, *Electric Machine in Electric & Hybrid Vehicle Application*, Proceeding of ICPE, 95, Seoul, pp 627--635.

[7] M.Ehsani, *Electrically Peaking Hybrid System And Method*, U.S. Patent pending.

[8] J. Howze, M. Ehsani and D. Buntin, *Optimizing Torque Controller for a Parallel Hybrid Electric Vehicle*, U.S. Patent pending.
[9] Proceedings of the ELPH Conference, Texas A&M University, College Station, Texas, Oct. 1994.

960448

An Empirically Based Electrosource Horizon Lead-Acid Battery Model

Stephen Moore and Merhdad Eshani
Texas A&M Univ.

ABSTRACT

A empirically based mathematical model of a lead-acid battery for use in the Texas A&M University's Electrically Peaking Hybrid (ELPH) computer simulation is presented. The battery model is intended to overcome intuitive difficulties with currently available models by employing direct relationships between state-of-charge, voltage, and power demand. The model input is the power demand or load. Model outputs include voltage, an instantaneous battery efficiency coefficient and a state-of-charge indicator. A time and current dependent voltage hysteresis is employed to ensure correct voltage tracking inherent with the highly transient nature of a hybrid electric drivetrain.

INTRODUCTION

The behavior of a battery in the hybrid electric vehicle enviroment is complex and demands detailed analysis of battery characteristics. Lead-acid battery behavior is notorious for its dynamics under load conditions and varying state of charge levels. Because of these peculiar dynamics, a transient lead-acid battery model must be based on a series of detailed experiments executed at varying state of charge conditions and power levels. In addition, experiments must be run to evaluate charging transients as well, due to the peaking properties of the hybrid electric drive train.

The battery model is a critical component in the simulation of a hybrid electric drive train. With current lead-acid battery technologies, on which the ELPH model is based, the battery must be treated with special care to not damage cycle life by avoiding deep discharge, over-charging and gassing [1]. These limitations make the battery's operating region fairly narrow. The battery must unfailingly supply peaking power each time it is called upon and must be able to accept charge back to prepare for the next transient. This peaking/charging cycle is very demanding on the battery and must stay within the battery's narrow operating bandwidth to avoid damage. This special care treatment must be considered when modeling the drive train.

Under the hybrid peaking philosophy, it must also be considered that the battery is completely responsible for vehicle performance during transient situations. The battery must provide large amounts of energy in short bursts and must recover as much energy as possible when charging opportunities exists. Wild voltage swings occur with the massive power demands, resulting in difficult to predict performance. These high power effects must be modeled with confidence to give the simulation realistic transient performance results.

HISTORIC AND AVAILABLE BATTERY MODELS

The most basic battery model is based on the electrochemistry of the lead-acid reaction. From these equations one can derive energy storage and electromotive forces given reactant masses and geometries. Unfortunately, the basic electrochemical reaction equations do not take into account thermodynamic or quantum effects that result in phenomenons such as the time rate of change of voltage under load. It is because of these extremely complex processes that most battery models are empirical rather than based on first principle.

The Peukert equation can be used to estimate state of charge and make a fairly confident battery model. Peukert's

equation simply states that the battery capacity decreases with increasing current [2,3]:

(1) $K = I_n - T_i$

(2) $QD = K \times I^{-(n-1)}$

Where QD is the capacity of the battery in Ampere-hours, dependent on current I and battery constant n. The constant n is usually n = 1.35 for lead-acid battery types. T_i is the amount of time to discharge at current I. For example, if I is increased, QD will decrease. The problem with this equation is that it cannot model variable rate discharges, intermittent discharges or voltage behavior. It is only a fixed-rate state of charge estimator.

There are several models available that use electrical circuit equivalents to predict battery performance. Two of these models, the Kleckner Model and the Zimmerman-Peterson model uses capacitors as charge storing elements. The Kleckner model is limited because it is a discharge only model. Also complicating the use of this model is that its electrical equivalent equation terms must be recalculated and updated every time the instantaneous current draw changes. [4]

The most widely known and used model is the Shepherd model. This empirical model is used in conjunction with the Peukert equation to obtain battery voltage and state of charge given power draw variations [5,6,7]:

(3) $E_T = E_s - Ri - Ki\dfrac{Q}{Q - \int idt}$

Where Q is the capacity of the battery in Ampere-hours, E_S is the open circuit voltage, Ri is the internal resistance, K_i is the polarization resistance, and $\int idt$ is the accumulated Ampere-hours. E_T is the battery terminal voltage. The capacity Q and instantaneous current i are then related to the Peukert equation to derive QD, fractional state of charge. State of charge is found by Q / QD * 100%. Notice that this model has a interdependence of battery voltage, current draw and state of charge, very like a real battery displays. The Shepherd model has been improved upon with the addition of extra terms to describe additional phenomenon, such as the improved internal resistance calculations afforded by the Lindstorm model. The Wood model incorporates secondary equations to describe overcharging and gas generation, along with a self discharge term which is not insignificant given the current lead acid battery technology.

Another widely used battery model is the fractional discharge model. This model is based on the premise that as capacity changes with current demands the peak power availability changes as well. This can be observed directly from the Shepherd model by observing the voltage and current as the capacity decreases. However, the fractional discharge model derives state of charge directly from the incremental power and energy densities rather than comparing capacities. This is a very intuitive way of obtaining the state of charge because the experiments required to analyze the power and energy densities are relativity easy. Experiments are run at several different state of charge levels and loads, and as the data points are collected they are curve fit to form an equation for power density. The results of this model do not include specifics about voltage and current but rather only power and state of charge. [8]

ELPH 2.0 BATTERY MODEL

The ELPH 2.0 battery model is a combination of the battery modeling techniques described above. Experiments similar to the ones required by the fractional state of charge model were run to characterize battery performance. Batteries were subjected to varying degrees of load at specific state of charge conditions. Using experimental results from several batteries, important relationships were developed. This model is based on results from more than a single sample to eliminate the possibility of modeling manufacturing aberrations in a single example from the manufacturer.

Key relationships used in constructing the model includes the voltage dependence on current draw and state of charge. A high confidence voltage modeling is a requirement of the ELPH simulation. Another key relationship is the battery efficiency's dependence from power draw and state of charge. According to Peukert's equation, at high currents the battery energy capacity will decrease more than the amount of energy removed. The difference between the change of amount of available energy and the amount of energy removed can be expressed as an efficiency. Battery efficiency is described as:

(4) $\eta = \dfrac{\Delta QD}{E_T \times i \times \Delta T}$

Where η is efficiency, ΔQD is the change of battery capacity, E_T is the battery voltage at the terminals, i is the instantaneous current, and ΔT is the time step. Notice that E_T * i * ΔT is energy. This equation can be rewritten as:

(5) $\eta = \dfrac{\text{energy capacity decrease}}{\text{energy removed}}$

Through experimentation, a mathematical surface consisting of a grid of measured data points was constructed. An equation was surface-fitted to these points, resulting in a η(SOC,P) relationship where η is efficiency, SOC is the state of charge, and P is the instantaneous power demand.

The next relationship developed is the E_T(SOC,i) relationship, describing the terminal voltage of the battery E_T given a current draw and the state of charge. Measured data points were obtained by subjecting the battery to several tests under different loads and state of charge conditions while monitoring voltage. Again, a mathematical grid was constructed and an equation was surface-fitted (see Figure 1 and 2 for characteristic surfaces).

Horizon Discharge

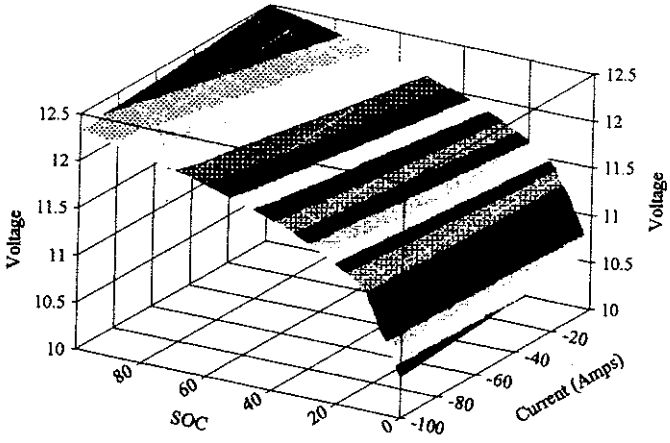

Figure 1. Notice that the voltage is nearly independent of current. This "flat" profile is very surprising and shows the Horizon's excellent suitability for electrically peaking applications.

Horizon Charge

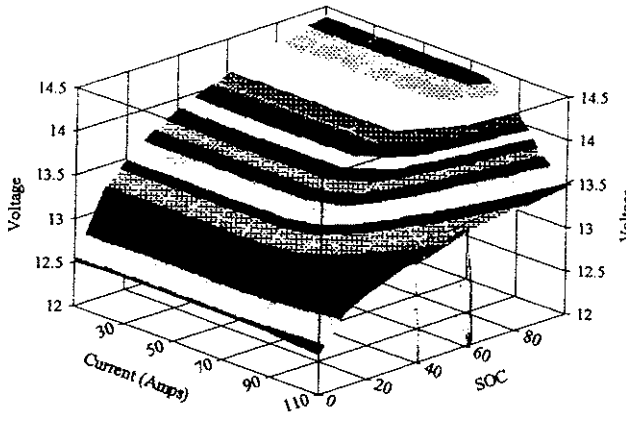

Figure 2. The recharge curve has the expected broad characteristic of being able to absorb large amounts of current at low states of charge.

A battery does not exhibit an instantaneous change in voltage with change of load. This differential change of voltage over time ($\Delta E_T/\Delta T$) had to be taken into account because the ELPH model requires very rapid peaking transients with extreme power demands. Inaccurate voltage modeling would lead to poor performance predictions. Most models that take this voltage hysteresis into account generalize the time constant to be about $\tau = 0.08$ seconds. After experimental measurements were made, a fixed time constant τ could not be assumed, rather the $\Delta E_T/\Delta T$ is variable, dependent on power demand. At low or near zero currents, the battery can take several seconds to approach a steady voltage. At high power demands, the battery voltage reacts much more quickly:

$$(6)\ \tau = f(\Delta T, i)$$

$$(7)\ E_T^{\bullet} = E_T \times e^{-\frac{\Delta T}{\tau}} + E_T(SOC,i) \times (1 - e^{-\frac{\Delta T}{\tau}})$$

This allows the voltage to track power demands with a hysteresis with a current dependent variable time constant (Figure 3)

The ELPH battery model operates by combining each of these terms to calculate terminal voltage and state of charge given a current demand. Outputs from the model include battery voltage Es, instantaneous current demand i, instantaneous power demand, battery efficiency η, $\Delta E_s/\Delta_T$ monitoring and state of charge SOC.

10 Second 5 kW Spike

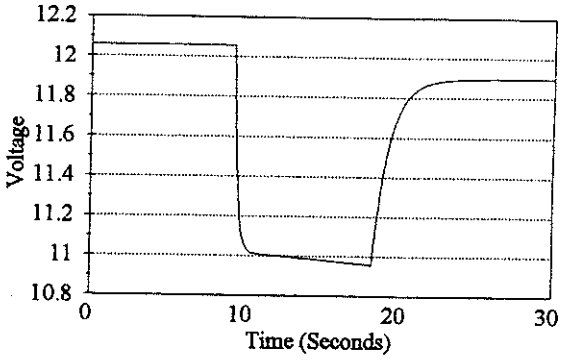

Figure 3 Voltage Hysteresis

MODEL LIMITATIONS

The current revision of the ELPH 2.0 battery model is capable of performing simulations of an Electrosource Horizon 95 Ampere-hour battery. Simulations have a number of restrictions to be eliminated in future revisions.

A major limitation to the present revision is that the charge equation relating efficiency to power demand and state of charge η(SOC,P) can be made more accurate. This is due to the difficulty of experimentation and available resources. With the advent of the ELPH stationary and mobile testbeds, this phenomenon will be readily observable in a vehicle environment, facilitating much more pertinent data and empirical measurements. The next revisions are expected to predict charging performance much more confidently.

Secondary equations that include battery inefficiencies such as heat and gas generation will also be added. The current revision of the model does not allow for overcharging, which imposes the restriction that the model must never experience charging conditions once the battery is fully charged. This problem must also be addressed because the hybrid electric drive train will expose the batteries to charging extremes as well as discharging extremes.

CONCLUSION

The ELPH 2.0 battery model is capable of high confidence performance prediction under a restricted operating bandwidth. The model takes into account variable efficiencies of charging and discharging under different and instantaneous situations, critical in a hybrid peaking drive train. State of charge is accurately predicted and overall battery efficiency over particular load scenarios can be calculated.

Battery voltage tracking is maintained by implementing a variable hysteresis dependent on current draw. Peak power and power density characteristics can be properly calculated, otherwise vehicle performance prediction would be skewed due to excessive or deficient power availability from the battery.

During the summer of 1994 the ELPH research team was awarded a 1994 Dodge Neon for the 1995 HEV Challange. The stock engine was removed and replaced by a parallel drivetrain consisting of a Honda CV250 motorcycle engine modified for compressed natural gas and an Advanced DC eight inch motor. Ten Electrosource Horizon batteries supply electrical power to a standard Curtis DC motor controller with regenerative capability. The control strategy, implemented by an Alan-Bradly programmable logic controller, was developed by the ELPH team during modeling and simulation studies. The vehicle is currenly being outfitted with a comprehensive data aquasition system to collect the neccesary data for model validation. With the accession of the ELPH mobile testbed, numerous improvements can be made to the model with the amount of data that will be available from an in-vehicle prototyping platform.

A stationary testbed consisting of electrical drive components will provide high precision data for further model validation. The stationary testbed features a 7.5 kW vector controlled induction motor connected in series with a 11 kW DC dynamometer. Power is supplied by a 144 volt battery pack. The DC dynamometer will be programmed with vehicle dynamics to simulate a road load. This testbed, expected to demonstrate electric vehicle driving scenarios by January 1996, will provide data on the performance of electric motors and batteries in EV and HEV environments.

ACKNOWLEDGMENT

The financial support of Texas A&M University, Texas Transportation Institute and Texas Higher Education Coordinating Board Advanced Technology Program for the work done in the ELPH project is gratefully acknowledged.

REFERENCES

1. Eshani, M., *et al.*, "Executive Summary of the ELPH Project", ELPH Conference Proceedings, 1994
2. White, K.E., "A Digital Computer Program for Simulating Electric Vehicle Performance", SAE 780216, 1978
3. Van Donegan *et al.*, "Theoretical Prediction of Electric Vehicle Energy Consumption and Battery State of Charge During Arbitrary Driving Cycles", EVC Symposium VI, EVC paper 8115, Baltimore, Oct. 1981
4. W. Facinelli, "Modeling and Simulation of Lead Acid Batteries for Photovoltaic Systems", Proceedings of the 18th IECEC, 1983
5. Unnewehr, L.E., and Freedman, R., "A Comparative Evaluation of Battery Models for Electric Vehicle Simulation", Industry Application Society Conf., 1979, IEEE IAS 79-31B
6. Shepherd, C.M., "Design of Primary and Secondary cells: An Equation Describing Battery Discharge", J. Electrochemical Soc., 1965, 112, pp. 644-657
7. Taylor, D.F., and Siwek, E.G., "The Dynamic Characterization of Lead Acid Batteries for Vehicle Applications", SAE 730252, 1973
8. Bumby, J.R, Forster, I., *et al.*, "Computer Modeling of the Automotive Energy Requirements for Internal Combustion Engine and Battery Electric Powered Vehicles", IEEE Proceedings, Vol 132, Pt. A, No. 5, Sept. 1985

OTHER REFERENCES

1. Manwell, J.F., and McGowan, J.G., "Lead Acid Battery Storage Model for Hybrid Energy Systems", Solar Energy, Vol. 50, No. 5, pp. 399-405, 1993
2. Salameh, Z.M., *et al.*, "A Mathematical Model for Lead-Acid Batteries", IEEE Transactions on Energy Conversion, Vol. 7, No. 1, March 1992, pp. 93-97
3. Hornstra, F., and Yao, N., "Standard Test Procedures for Electric Vehicle Batteries at the National Battery Test Laboratory", SAE Paper No. 820401, 1982

ABOUT THE AUTHOR

Stephen Moore is an electrical engineering graduate student at Texas A&M University doing research for the ELPH team under the supervision of Dr. Merhdad Ehsani. His main area of focus is computer modeling and simulation of energy storage systems. The ELPH team can be reached by FAX at 409-862-1976.

Design Considerations For EV And HEV Motor Drives

Khwaja M. Rahman
Student Member, IEEE

Mehrdad Ehsani
Fellow, IEEE

Texas Applied Power Electronics Center
Texas A&M University
College Station, TX 77843-3128
Tel: (409) 845-7582
Fax: (409) 862-9173
Email: ehsani@ee.tamu.edu

Abstract: Vehicle load dictates an extended range constant power operation from its propulsion system in order to meet its operational constraints such as initial acceleration, gradability etc., with minimum power rating. The internal combustion engine (ICE) fails miserably in generating this torque profile. Multiple gearing, therefore, is necessary with the operation of the ICE for vehicle application. An indefinite extension of the constant power range, however, has some undesirable effects on the overall system. The total system cost may go up with the extension, beyond a certain point, of the constant power range. It may be possible, for each motor type and its design, to arrive at some optimal number for the extended constant power range which will minimize the total system cost. To help in obtaining the extended constant power range special design and control of the electrical propulsion system would be necessary. This design process would include selection of motor type, its size, maximum speed, control strategy etc. This paper will discuss the necessity of the extended constant power range and its effect on the system. The relevant electric motor design and control issues will be discussed. Several commonly used motors, with special emphasis given to switched reluctance motor (SRM), will be studied to determine their performances for vehicle applications.

I. Introduction

Electric and hybrid electric vehicles offer the most promising solutions to reduce vehicular emission. Electric vehicle (EV) constitute the only commonly known group of automobiles that qualify as zero emission vehicles (ZEVs). These vehicles use an electric motor for propulsion, and batteries as electrical energy storage devices. Although, there have been significant advancements in motors, power electronics, microelectronics, and microprocessor control of motor drives, the advancement in battery technology has been relatively sluggish. Hence, the handicap of short range, associated with EV's still remains. Given these technology limitations, hybrid electric vehicle (HEV) seems to be the viable alternative to ICE automobile at the present. HEVs qualify as ultra low emission vehicles (ULEVs), and do not suffer from the range limitations imposed by the EVs. These vehicles combine more than one energy source to propel the automobile. In the heat engine/battery hybrid systems, the mechanical power available from the heat engine is combined with the electrical energy stored in a battery to propel the vehicle. These systems also require an electric drive train to convert electric energy into mechanical energy, just like the EV. Hybrid electric system can be broadly classified as series or parallel hybrid systems.

In series hybrid systems, all the torque required to propel the vehicle is provided by an electric motor. In parallel hybrid systems the torque obtained from the heat engine is mechanically coupled to the torque produced by an electric motor [1]. In the electric vehicle, the electric motor behaves exactly in the same manner as in a series hybrid. Therefore, the torque and the power requirements of the electric motor are roughly equal for an EV and series hybrid, while they are lower in parallel hybrid.

Designing an electrical propulsion system for EV and HEV is a difficult job. Special design and control of a motor would generally be required in order to optimize its performance for vehicle applications. An extended constant power range operation is necessary from the electric motor to minimize the acceleration power of the vehicle. This paper will discuss this necessity of the extended constant power range and its effect on the propulsion system. The design and control issues for extending the constant power range of operation for few commonly used motors will be discussed with paying special attention to the switched reluctance motor.

II. Optimal Torque Speed Profile of the EV and HEV Propulsion System

Our recent study has shown that, a vehicle, in order to meet its operational constraint such as initial acceleration and gradability with minimum power needs its propulsion system to operate in constant power [2]. The power rating of the motor that is deviating from the power source regime can be as much as two times that of a motor operating in constant power through out its speed range in a vehicle. Fig. 1. represents theoretically the optimal torque-speed profile of any motor drive for vehicle application.

The importance of the extended constant power range can be better understood by a numerical example comparing the required acceleration power for different constant power speed range (as a multiple of its base speed). Let us consider the following vehicle:

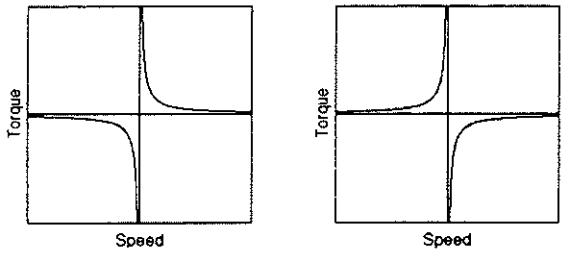

(a) (b)

Fig. 1. Optimal torque-speed profile for EV and HEV propulsion systems, (a) motoring, (b) generating.

- 0-26.82 m/s (0-60 mi/h) acceleration in 10 s;
- vehicle mass of 1450 kg;
- rolling resistance coefficient of 0.013;
- aerodynamic drag coefficient of 0.29;
- wheel radius of 0.2794 m (11 in);
- level ground;
- zero head-wind velocity;
- maximum motor speed 10,000 r/m;
- maximum vehicle speed 44.7 m/s (100 mi/h);

Table I shows the example of power requirement to meet the above acceleration requirements for several

Table I

	Constant Power Range					
	1:1	1:2	1:3	1:4	1:5	1:6
Motor Rated Power (kW)	110	95	74	67	64	62

constant power ranges of the propulsion power train. The result of Table I clearly shows the importance of extended constant power range. The electric motors capable of performing longer constant power ranges meet the acceleration requirement with lower power rating. A detailed study of the propulsion system design of EV and HEV can be obtained in [2]. Fig. 2 shows the power rating of the propulsion system for the required initial acceleration as shown in Table I. however, as a function of the motor rated speed. The power requirement is minimum as we can see in Fig. 2 when the motor rated speed is zero, i.e. the operation is entirely in constant power. The other extreme of the curve shows the power requirement for operation of the propulsion system entirely in constant torque.

We have already seen that the longer constant power range of operation of the electrical propulsion system reduces the power requirement for initial acceleration. However, with the increase of the constant power range of the electrical motor, for the same maximum speed of the motor, the rated torque of the motor increases despite the fact that motor power is decreasing. This is illustrated in Fig. 3 for a motor with maximum speed of 10,000 rpm. Therefore, although the converter power (volt-ampere) requirement hence the converter cost will decrease with increasing constant power range, the motor size, volume, and

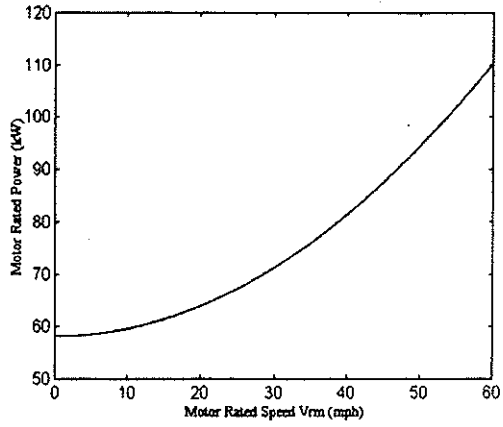

Fig. 2. Initial acceleration power requirement.

cost will increase with increasing constant power range. The motor size can only be reduced in this case by picking a

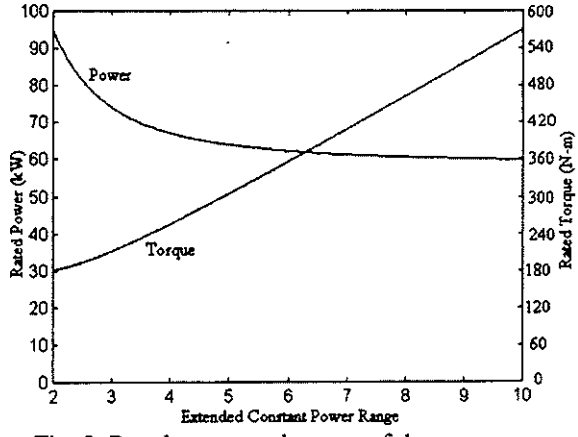

Fig. 3. Rated power and torque of the motor as a function of the constant power speed range.

motor capable of running at a higher speed. The motor maximum speed, in one hand, can not be increased indefinitely without incurring more cost. On the other hand, high maximum motor speed would require a bigger transmission. Hence, there exist multitude of system level conflicts with the extension of the constant power range. However, for different motor (different motor has different high speed capability) it may be possible to arrive at an optimal constant power range number base on the cost and the performance analysis. This analysis is, however, beyond the scope of this paper.

III. Design Considerations for EV and HEV Motor Drives

In light of the above discussion we would expect the following characteristics from EV and HEV motor drives

- a wide speed constant power range
- high maximum speed capability
- good efficiency
- low cost
- low maintenance
- safety/reliability
- ease of control

Modern electric motor is benefited from design and material innovations. Availability of low loss, high grade, stress relieved, coated electrical steel laminations have contributed significantly to the improvement of efficiency and reduction in size of modern electric motors. In the recent EVs and HEVs the dc commutator motors, ac induction motors, and permanent magnet (PM) brushless dc motors are common. Recently, there is also an interest in using switched reluctance motor.

Two most important characteristics for the EV and HEV motor drives are the wide speed constant power capability and the high operational efficiency. Efficiency is particularly important for the operation of the electric vehicle. The electric machines for electric and hybrid electric vehicle applications should be designed and controlled for better efficiency. For instance, the high speed operation of the motor would increase the iron losses. Motors for vehicle application should, therefore, be designed with very thin laminations. As far as the efficiency is concerned, the permanent magnet motors have an upper hand over all other motors. The absence of rotor winding eliminates the rotor losses. Furthermore, due to the presence of the permanent magnet field, the rotor excitations are not required to be fed through the stator as are the cases for the induction and the switched reluctance motor. However, at speeds beyond the base speed weakening of the permanent magnet field requires an additional stator current component. This would lower the efficiency of the permanent magnet motors at higher speeds. Switched reluctance motors can be also designed and controlled for improved efficiency. For example, motors designed with narrower stator pole widths will have more room for winding placement. This would result in a lower copper loss. However, other impacts for this simple modification should be studied.

Extended constant power capability, on the other hand, is motor type, its design, and the control dependent. DC commutator motors are inherently suited for extended constant power operation. However, poor efficiency, low maximum speed capability, and bulky nature limit their operation in vehicle applications. The constant power capability of ac motors depends largely on the motor type its design and also on the control strategy. The design and control issues for obtaining an extended constant power range are discussed next for few potential EV and HEV motors.

A. Induction Motor

The control of induction motor for EV and HEV applications is predominantly the field oriented control (FOC) [3]. Break down torque in induction motor, however, limits their extended speed constant power capability. A machine designed with a high breakdown torque, e.g. four times the rated torque, allows a constant power range of four times the base speed. The constant power range, therefore, can be extended by designing motor with a high breakdown torque. Induction motors designed with lower leakage inductance have higher breakdown torque. This method of designing an induction motor was presented by Boglietti [4] for spindle application. Induction motor designed with low leakage inductance, however, has higher harmonic components and experience more copper loss. Two other methods of control of induction motor are also presented which extend the constant power range. One method involves magnetic contacts and tapping in the windings [5]. As the speed increases beyond the base speed, the magnetic contacts are used with the tappings to progressively cut some part of each phase windings. This way the back emf is reduced and a long constant power range is obtained. The other method involves the winding pole changing. By changing the winding connection a four pole winding can be changed to a two pole winding and a designed constant power range of two times the base speed can be extended, in theory, to four times the base speed. Most recently [6], a contactor less pole changing scheme is presented which uses two inverters with the two sets of winding of the induction motor. By changing the direction of current flow in one of the windings, four pole winding configuration is changed to a two pole configuration and vice versa.

B. Permanent Magnet ac (PMAC) Motor

Two types of permanent magnet motors are generally built. One is the trapezoidal back emf type while the other is the sinusoidal back emf type. The trapezoidal motors usually have magnets mounted on the surface. The surface mounting of the magnets reduces the stator inductance. As a consequence, these motors suffer from poor field weakening capability. By adding external inductance and then by the usual phase advancing technique the range can be extended [7]. The additional cost and the bulkiness make this method not very attractive. A specially designed multi-pole multi-phase trapezoidal motor which claims to eliminate the phase coupling, has been demonstrated to obtain a range of three times the base speed [8].

The sinusoidal PM motors designed with salient rotor by the interior magnet placement are capable of exhibiting an extended constant power range. Some design rules for sinusoidal PM motors and the synchronous reluctance motor for obtaining a long constant power range were presented in [9]. An optimal design line as functions of rotor saliency and magnet usage was also presented. As mentioned there, the key to obtaining a long constant power range is to design the rotor with high saliency, if one wants to minimize the magnet usage. The high saliency rotors are, however, usually axially laminated. Hence, the rotor construction will be costly, moreover, the rotor will have speed limitations.

C. Switched Reluctance Motor (SRM)

The SRM relies upon reluctance torque rather than the more conventional reactive torque of wound field synchronous, surface magnet PM, and induction machines. The SRM is a doubly salient reluctance machine with independent phase windings on the stator. The rotor does not have any winding, and is usually made of steel lamination. The stator and rotor have unequal number of poles with three phase 6/4, four phase 8/6, and three phase 12/8 being common configuration. Due to the absence of rotor windings this motor is very simple to construct, has low inertia, and allows an extremely high speed operation. A cross sectional view of a 6-4 SRM is shown in Fig. 4.

The absence of rotor copper loss eliminates the problem, as in an induction motor, associated with rotor cooling which has a poor thermal path. Moreover, due to unipolar excitation, the SRM core is subjected to a magnetic reversal at a much reduced frequency than the stator excitation. This results in a reduced hysteresis loss in the SRM core unlike the permanent magnet (PM) motors and the induction motor.

SRMs normally are low cost machine for their extremely simple construction. Moreover, due to the unipolar excitation, it is possible to design SRM converters which requires a minimum of one switch per phase. SRM operation is extremely safe and this motor is particularly suitable for hazardous environment. The SRM drive produces zero or small open circuit voltage and short circuit current. Furthermore, most SRM converters are immune from shoot through faults, unlike the inverters of induction and brushless dc motors.

Rapid acceleration and extremely high speed operation in SRM is possible for its low rotor inertia and simple construction. SRM operates in constant torque from zero speed upto the rated speed. Above rated speed upto a certain speed, the operation is in constant power. The range of this constant power operation depends on the motor design and its control. Beyond constant hp operation and up to the maximum speed, the motor operates in the natural mode, where the torque reduces as the square of the speed. Because of this wide speed range operation, SRM is particularly suitable for gearless operation in EV/HEV propulsion.

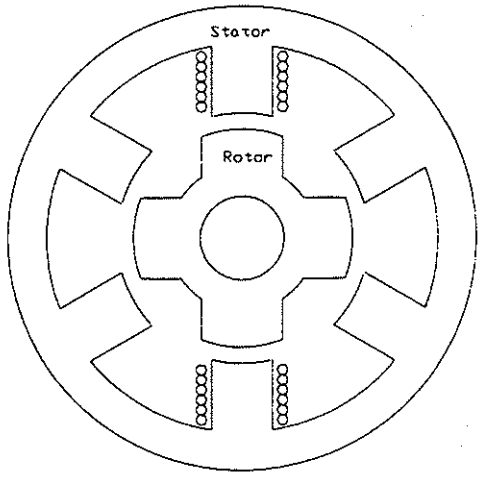

Fig. 4. Cross sectional view of a 6-4 SRM.

Motor current in the SRM drive below base speed can be controlled from zero to the maximum by chopping with a fixed phase excitation. The excitation angle can be controlled to optimize efficiency and torque ripple. Operation beyond base speed in constant hp is possible by phase advancing the firing angle until an overlapping between the two successive phases occurs.

To extend the constant power range the motor should be designed appropriately and controlled optimally. In order to obtain the optimal control parameters which maximize the constant power range it is necessary to obtain an accurate model of SRM. The highly non-linear nature of operation of SRM, however, complicates the analysis. The non-linear field solutions within the motor are needed to be solved in order to

develop a non-linear model of SRM. For accuracy, finite element (FE) analysis should be performed for the field solutions. The design methodology presented next may be followed in order to obtain an appropriate SRM geometry for EV and HEV applications.

1. SRM Design Methodology

The design methodology suggested in this paper has the following steps

i) Designing, using hand calculation, of several SRM with varying stator and rotor pole numbers and geometries.

ii) Investigation of the static performance characteristics of each SRM designed geometries using finite element analysis.

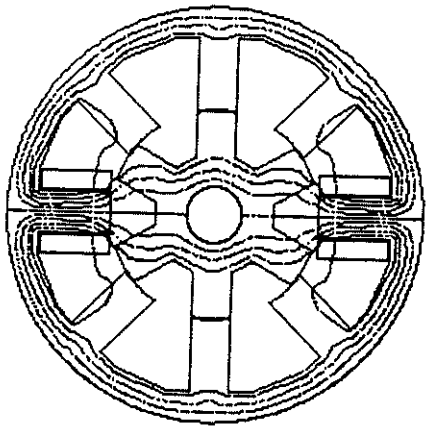

Fig. 5. A 2-D finite element field plot for an 8-6 SRM.

iii) Development of a non-linear SRM model using the generated static flux linkage and torque characteristics.

iv) Development of an optimal control scheme using the dynamic model. More about the optimal control algorithm will be discussed later.

v) Investigation, using the dynamic model, the steady state and dynamic performance of each SRM geometry with the optimal control.

vi) Repeat step i) through v) until the desired performance is achieved.

The desired performances for EV and HEV motors have been discussed earlier. We are more concerned here to obtain a long constant power range. The proposed design methodology is a powerful approach to investigate the SRM capability for EV and HEV applications, however, is extremely time consuming. We next talk about the non-linear modeling of SRM and development of the optimal control algorithm.

2. SRM Non-linear Model

The SRM voltage equation is

$$V = iR + \frac{d\psi}{dt} \quad (1)$$

where i is the phase current, R is the phase coil resistance, and ψ is the flux linkage. $\psi(i,\theta)$ is a nonlinear function of phase current i and the rotor position θ. The finite element analysis can be used to obtain the non-linear solution of the $\psi(i,\theta)$. One such static solutions of the non-linear field and the developed torque are shown in the Fig. 6.

These static flux (Ψ-θ-i) and torque (T-θ-i) data are used to develop a dynamic model of SRM. A block diagram of the dynamic model is shown in Fig. 7.

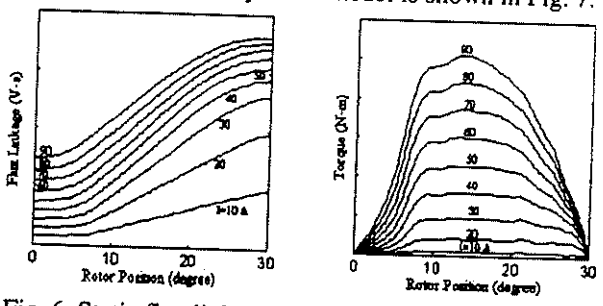

Fig. 6. Static flux linkage and the torque as functions of rotor position and stator current.

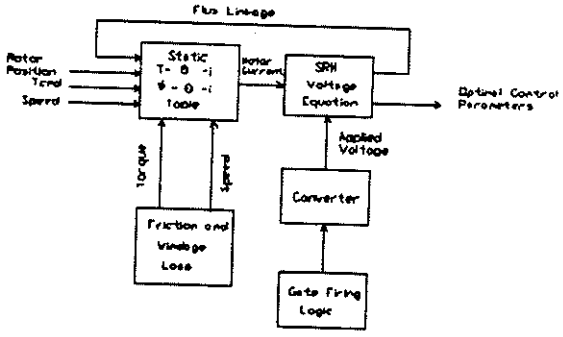

Fig. 7. A block diagram of the non-linear model of SRM.

SRM experience much higher commutation frequency than other motors of same speed and pole counts. Moreover, the flux waveform at different core and pole segments of SRM have different frequencies and different shapes, rich in harmonics. As a consequence, the core loss at high speed can very well become the dominant loss component in the motor. Therefore, for better accuracy the core loss model should be included in the dynamic model. Due to the non-linear and non-sinusoidal nature of operation, development of the core loss model is difficult for SRM, nonetheless, core loss models are presented in the literature [10,11]. The developed dynamic model is used to obtain the optimal control parameters which will

maximize the constant power range with maximum torque per ampere.

3. Optimal Control Algorithm

SRM high speed control parameters are the

- phase turn-on angle.
- phase turn-off angle.

these control parameters need to be controlled optimally to extend the constant power range with maximum torque per ampere. The developed non-linear model is used in this purpose. The necessary process is a search process or a root seeking process which will examine all the possible control parameters for each torque and speed to obtain the optimal ones. As can be understood, this is also a time exhaustive process.

4. Design Example

One 30 kW 6-4 SRM design along with its steady state performance with the optimal control will be presented in this sub-section. The presented SRM design is one design, not necessarily the SRM design, however, the constant power range performance is quite impressive for the presented SRM. A more systematic study of the SRM design methodology will be presented elsewhere.

Design Geometry:

- Power 30 kW
- Bus voltage 270 V
- Corner Speed 2500 rpm
- Peak torque, 114.6 N-m
- Maximum Speed 12,500 rpm
- Rotor pole angle 32.5°
- Stator pole angle 31°
- Air gap 0.04 inch
- Rotor outer diameter, 5.7 inch
- Stack length, 5.7 inch
- Stator inner diameter, 8.6 inch
- Stator outer diameter, 10.5 inch
- Number of turns per pole, 30
- RMS phase current, 104 amps (4 A/mm^2)
- M-19 steel, 14 mill thickness

The average torque along with the optimal angles are shown in Fig. 8. The phase current at high speed is shown in Fig. 9. As we can see the, the phase current decreases during constant power high speed operation, when controlled optimally. This is a direct consequence of the fact that the power factor is increasing during the high speed operation of the SRM.

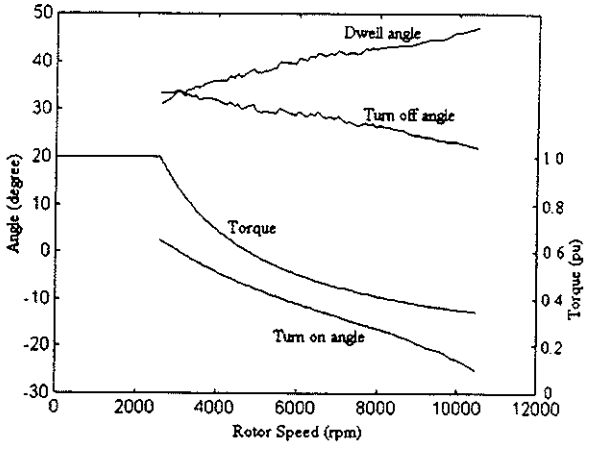

Fig. 8. Average torque and the optimal angles for high speed operation of SRM.

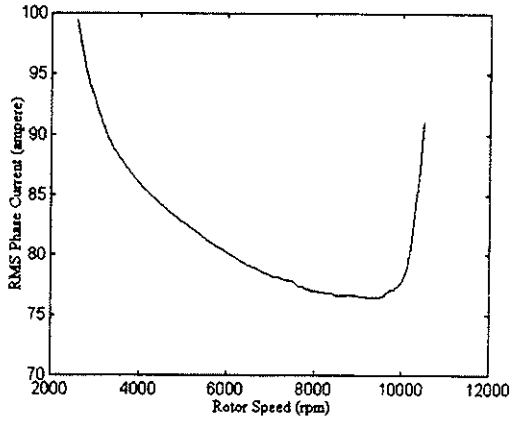

Fig. 9. Phase current during high speed constant power operation.

IV. Conclusion

The extended range constant power capability of different motors are discussed. Different means to extend the constant power range are also discussed. The design methodology and the control strategy for obtaining an extended constant power range for SRM are presented. The presented SRM design shows a good constant power range with improved power factor over its low speed operation.

V. References

[1] A. F. Burke, "Hybrid/Electric vehicle design options and evaluations," *SAE paper # 920447*, Feb., 1992.

[2] M. Ehsani, K. M. Rahman, and H. Toliyat, "Propulsion system design of electric and hybrid vehicles," *IEEE Trans. on Industrial Electronics*, vol. 44, no. 1, pp. 19-27.

[3] A. M. Trzynadlowski, *The Field Orientation Principle in Control of Induction Motors*, Kluwer Academic Publishers, Boston, 1994.

[4] A. Boglietti, P. Ferraris, M. Lazzari, and F. Profumo, "A new design criteria for spindle induction motors controlled by field oriented technique," *Electric Mach., Power Syst.*, vol. 21, pp. 171-182, 1993.

[5] T. Kume, T. Iwakane, T. Sawa, and T. Yoshida, "A wide constant power range vector-controlled ac motor drive using winding changeover technique," *IEEE Trans. on Industry Applications*, vol. 27, no. 5, Sept./Oct. 1991.

[6] M. Osama, and T. A. Lipo, "A new inverter control scheme for induction motor drives requiring wide speed range," *IEEE Trans. Industry* Applications, vol. 32, pp. 938-944, 1996.

[7] T. Sebastian and G. R. Slemon, "Operating limits of inverter-driven permanent magnet motor drives," *IEEE Trans. Industry Applications*, vol. 23, pp. 327-333, 1987.

[8] C. C. Chan, J. Z. Jiang, G. H. Chen, X. Y. Wang, and K. T. Chau, "A novel polyphase multiple square-wave permanent magnet motor drive for electric vehicles," *IEEE Trans. on Industry Applications*, vol. 30, no, 5, pp. 1258-1266, Sept./Oct. 1994.

[9] W. L. Song, and T. J. E. Miller, "Field weakening performance of brushless synchronous AC motor drives," *IEE Proc. Electric Power Application*, vol. 141, no. 6, pp. 331-340, 1994.

[10]